Research Square

Preprints are preliminary reports that have not undergone peer review.
They should not be considered conclusive, used to inform clinical practice,
or referenced by the media as validated information.

Genome-wide Transcriptomic Analysis Reveals Acid Stress-Responsive Toxin-Antitoxin System in Helicobacter pylori 26695

Deepak Kumar Behera
University of Delhi
Madhu Yadav
University of Delhi
Nidhi Gupta
TERI University
Vijay Kumar Verma
vijayverma@south.du.ac.in

University of Delhi

Research Article

Keywords: Helicobacter pylori, Toxin-antitoxin System, pH/acid Stress, RNASeq, Bacterial persistence, Gastric pathogen gene regulation

Posted Date: September 3rd, 2026

DOI: https://doi.org/10.21203/rs.3.rs-10639790/v1

License: This work is licensed under a Creative Commons Attribution 4.0 International License.
Read Full License

Additional Declarations: No competing interests reported.

Abstract

Helicobacter pylori colonizes the human stomach and survives under highly acidic conditions, but the mechanisms underlying its persistence remain poorly understood. Toxin-antitoxin (TA) systems are stress-responsive modules associated with growth arrest and dormancy, but their role in *H. pylori* acid stress remains largely unexplored. Here, we characterized the transcriptomic response of 80 previously identified putative TA genes in *H. pylori* 26695 under acid stress using rRNA-depleted RNA sequencing and qRT-PCR validation. *H. pylori* cultures were exposed to pH 2.5 or 5.5 for 30 min and 4 h. At pH 2.5, nearly half of 1,564 annotated genes showed significant transcriptional changes, revealing an early response followed by adaptive recalibration. The 80 TA genes were enriched among acid-responsive transcripts and showed condition-dependent expression. Across 48 putative TA systems, toxin-dominant expression was observed in several families. Network analysis identified ParBC4, PhdDoc1, and NikR1 as highly connected hubs. These findings implicate putative TA systems in the acid stress response of *H. pylori*.

Key Points

• Genomewide rRNA-depleted RNA-seq identified acid-responsive transcriptional changes across 1,564 annotated genes of 26695, including enrichment of 80 putative toxin-antitoxin (TA) genes under severe acid stress (pH 2.5).

• Multiple TA families showed toxin-dominant expression under severe acid stress, while qRT-PCR validation of 40 TA genes demonstrated strong agreement with RNA-seq (Pearson = 0.928, < 0.0001).

• Network analysis identified ParBC4, PhdDoc1, and NikR1 as central regulatory hubs. Which suggests that TA systems form an integrated acid stress-responsive regulatory network in .

Introduction

Helicobacter pylori is a Gram-negative, microaerophilic bacterium that colonizes the human gastric mucosa. It is recognized as a Group I carcinogen by the International Agency for Research on Cancer (IARC) (**2012**). *H. pylori* affects approximately half of the world's population and associated with chronic gastritis, peptic ulcer disease, mucosa-associated lymphoid tissue (MALT) lymphoma, and gastric adenocarcinoma (Bauer and Meyer 2011; **Cover T. 2016**). Although possessing a relatively small genome i.e. ~1.67 Mb comprising ~ 1,564 protein-coding genes (Tomb 1997), *H. pylori* exhibits an extraordinary capacity to establish lifelong infection within the hostile gastric environment. Its successful and persistent colonization depends on multiple adaptive strategies that allow the bacterium to withstand continuously changing conditions encountered in the human stomach (Yang et al. 2023).

Acid tolerance represents one of the most critical determinants of *H. pylori* survival. The urease enzyme and the pH-gated urea channel UreI constitute the major acid resistance system and maintain periplasmic pH homeostasis through ammonia production (Scott et al. 2002). Additional mechanisms,

including arginase and aliphatic amidase pathways, outer membrane remodeling, and chemotactic responses, further contribute to adaptation under acidic conditions (Marcuset al. 2018; Wen et al. 2003). Exposure to acidic/low pH induces extensive transcriptional reprogramming affecting metabolic pathways, membrane proteins, motility, and virulence-associated genes (Marcus et al. 2018). In the pioneering differential RNA (dRNA) sequencing study, Sharma et al. (2010) identified 1,907 transcription start sites (TSS) and extensive antisense transcription throughout the *H. pylori* genome (Sharma et al. 2010). This highlights the complexity of transcriptional regulation in this pathogen. However, several stress-responsive mechanisms that contribute to long-term survival and persistence remain poorly understood.

Toxin-antitoxin (TA) systems are widespread genetic modules generally composed of a stable toxin and a cognate labile antitoxin. Under favourable growth conditions, the antitoxin neutralizes toxin activity. However, environmental stress promotes antitoxin degradation, releasing the toxin and modulating essential cellular processes (Jurėnas et al. 2022; Yamaguchi and Inouye 2011). TA systems are increasingly recognized as important regulators of stress adaptation and have been implicated in reversible growth arrest, metabolic slowdown, bacterial persistence, multidrug tolerance, and defence against bacteriophages (Jurėnas et al. 2022; Page and Peti 2016; Pandey and Gerdes 2005). Their toxins affect diverse cellular processes, including translation, DNA replication, membrane integrity, and cell wall biosynthesis, thereby facilitating bacterial survival under adverse conditions. Owing to their remarkable diversity and functional heterogeneity, the TA systems have emerged as important modulators of bacterial physiology and persistence.

Several characteristics of *H. pylori* suggest the existence of dormancy associated survival mechanisms. This bacterium can persist in the gastric niche for decades, frequently undergo morphological conversion into viable but non-culturable (VBNC) coccoid forms, and exhibits increasing rates of eradication failure worldwide (Reshetnyak and Reshetnyak 2017). Recent work also suggests that dormant *H. pylori* populations may contribute to recurrence and disease progression (Akbari et al. 2024). In many bacterial pathogens, TA systems have been implicated in persistence and stress tolerance. However, their physiological significance in *H. pylori* remains largely unexplored. To date, only a limited number of TA modules have been experimentally characterized in *H. pylori*. The type II TA pairs Hp0892-Hp0893 and Hp0894-Hp0895 were identified and structurally characterized by Han et al. (Han et al. 2013; Han et al. 2011). Further, the type I TA system i.e. AapA1-IsoA1 pair was shown to promote conversion of spiral shape bacteria into coccoid forms (El Mortaji et al. 2020). More recently, a YafQ family toxin encoded within the disease-associated integrative and conjugative element (ICE), tfs4 was reported to exhibit growth inhibitory activity (Boampong et al. 2020). These observations suggest that TA systems may contribute to stress adaptation and persistence in *H. pylori*. Although, their broader physiological roles remain unknown.

In our previous study, a comprehensive computational analysis using TADB, TASmania and Pfam domain searches predicted an extensive repertoire of putative TA loci in *H. pylori* 26695. The study suggested that these systems are considerably more abundant than previously appreciated (Gupta et al. 2022). The

predicted TA modules encompass diverse toxin families with putative functions in translation inhibition, membrane perturbation, DNA replication, and cell wall metabolism. However, the transcriptional behaviour of these putative TA systems under physiologically relevant stress conditions encountered during gastric colonization has not been investigated until now. Although several transcriptomic studies have examined acid-responsive genes in *H. pylori*, no genome-wide study has systematically explored the response of predicted TA systems to the acid stress.

In the present study, we performed rRNA-depleted RNA sequencing of *H. pylori* 26695 exposed to extreme (pH 2.5) and moderate (pH 5.5) acid stress at early and prolonged time points i.e. 30 min and 4 h respectively. Differentially expressed toxin-antitoxin genes and operons were further validated by qRT-PCR and analysed using network-based approaches. This study provides the first genome-wide view of acid-responsive toxin-antitoxin systems in *H. pylori*. This further, offers new insights into their potential roles in stress adaptation and persistent gastric colonization.

Materials and Methods

Helicobacter pylori culture and acid stress conditions

H. pylori 26695 was cultured under microaerobic conditions (5% CO_2, 37°C) on brain heart infusion (BHI) agar supplemented with 8% heat-inactivated horse serum (Sharma et al. 2009). For transcriptomic analyses, bacteria were grown in BHI broth supplemented with 8% horse serum at 37°C and 150 rpm for 48 hours until OD_{600} reached 0.9-1.0 (Blanchard and Nedrud 2006; Kim et al. 2025; Richards et al. 2011). Detailed growth kinetics are provided in supplementary data (**Fig. S1 & S2)**.

To mimic physiologically relevant gastric acid conditions encountered by *H. pylori* during colonization of the human stomach, cultures were exposed to pH 2.5 (extreme acid stress), pH 5.5 (moderate acid stress), and pH 7.4 (control). The media pH was adjusted using HCl immediately before stress induction. OD_{600} 0.9-1.0 cultures were resuspended in media adjusted to the respective pH conditions and incubated for 30 min and 4 h. Cells were harvested by centrifugation (2500 × g, 5 min, 4°C), and pellets were stored at -80°C until further processing for total RNA isolation.

Total RNA isolation and quality assessment

Total RNA was isolated from bacterial pellets (~ 10^8 cells) using the RNeasy Mini Kit (Qiagen) according to the manufacturer's instructions with minor modifications to improve integrated RNA recovery. Briefly, cells were lysed in RLT buffer supplemented with β-mercaptoethanol, followed by mechanical disruption. Residual genomic DNA was removed by one on-column DNase treatment (Qiagen) followed by two sequential TURBO DNase (Thermo-Fisher Scientific) treatments (Green and Sambrook 2019). Absence of genomic DNA contamination was confirmed by PCR amplification of the housekeeping gene *flaA* (Hp0601) (**Fig. S4)**. RNA concentration and purity were assessed using a NanoDrop spectrophotometer, while RNA integrity was evaluated by agarose gel electrophoresis (**Fig. S3)**. Samples with A260/A280 and A260/A230 ratios ≥ 1.8 were considered suitable for downstream analyses.

RNA sequencing and transcriptome analysis

RNA integrity was further assessed using Qubit fluorometry and Agilent TapeStation analysis (**Fig. S5)**. Ribosomal RNA (rRNA) was depleted from approximately 500 ng of total RNA per sample using the NEBNext rRNA Depletion Kit. Strand-specific libraries were prepared using the NEBNext Ultra II Directional RNA Library Prep Kit for Illumina and sequenced on the Illumina NovaSeq platform to generate paired-end reads. Raw RNA-seq reads have been deposited in the NCBI Sequence Read Archive (SRA) under BioProject accession PRJNA1505738.

Raw sequencing data were assessed using FastQC v0.12.1 (Andersson et al. 2010) and processed using fastp v1.0.1 (Chen 2023) to remove adapter sequences, low-quality bases, and short reads. High-quality reads were aligned to the *H. pylori* 26695 reference genome (RefSeq: NC_018939.1; GenBank: AE000511) using Bowtie2. Gene expression analyses were performed using the edgeR version 4.8.2 package, where raw counts were normalized using the trimmed mean of M-values (TMM) method and transformed to $\log_2$ counts per million (CPM) (Langmead and Salzberg 2012; Robinson et al. 2010). Differential gene expression analyses were performed by comparing each acid-stress condition with the corresponding pH 7.4 control at the same time point.

cDNA synthesis, operon validation, and quantitative real-time PCR

Total RNA was reverse transcribed using the Verso cDNA Synthesis Kit following the manufacturer's instructions. Co-transcription of selected toxin-antitoxin (TA) gene pairs were assessed using operon-specific PCR amplification. A list of TA operons was selected based on our previous bioinformatics analyses of *H. pylori* 26695 (Gupta et al. 2022). Primers for qRT-PCR targeting individual toxin and antitoxin genes and toxin-antitoxin junction regions were designed. Junction primers were designed with the forward primer positioned near the 3' end of the upstream gene and the reverse primer near the 5' end of the downstream gene to amplify the TA junction region. All primers were designed using NCBI Primer-BLAST with a strict amplicon size of 160–180 bp **(Fig. S15).**

Quantitative real-time PCR (qRT-PCR) was performed using SYBR Green chemistry. Reference genes (described in the results section) and control genes were selected based on previous experimental studies of acid stress responses in *H. pylori* (Ang et al. 2001; Loh et al. 2021; Marcus et al. 2018; Merrell et al. 2003). Reactions were performed in technical duplicates for each sample and its primer combination **(Supplementary Table S.1, S.2 & S.3)**. Relative gene expression was calculated using the 2^−ΔΔCt method, with the geometric mean of 16S and 23S rRNA used for normalization. Expression levels were determined relative to the corresponding pH 7.4 control samples.

Regulatory network construction and statistical analysis

Differential expression data obtained from qRT-PCR were used to construct co-regulatory interaction networks of TA genes and operons under different acid stress conditions. Network visualization and

topological analyses were performed using Cytoscape v3.10. Correlations between RNA-seq and qRT-PCR datasets were assessed using Pearson's correlation coefficient in Origin 2024 (Academic licence DUCC). Heat maps, scatter plots, bar graphs, violin plots, Sankey diagrams, and other data visualizations were generated using Origin 2024 and Python 3.13 using matlabplotlib/seaborn.

Results

Genome-wide transcriptional response of *H. pylori* 26695 under acid stress

To characterize the transcriptional response of *H. pylori* 26695 to acidic conditions, we performed rRNA-depleted RNA sequencing following exposure to moderate (pH 5.5) and extreme (pH 2.5) acid stress for 30 min and 4 h, using pH 7.4 as the corresponding physiological control (**Ang et al. 2001**; **Loh et al. 2021**; **Merrell et al. 2003**; **Zimmerman et al. 2023**). The transcriptional complexity of *H. pylori* has previously been demonstrated by the identification of 1,907 transcription start sites and 337 primary operons, with approximately 87.5% of annotated genes exhibiting transcriptional activity (**Sharma et al. 2010**). Here, using RNA sequencing, an average of 39.58 million paired-end reads and 6.29 Gb of raw data per library were generated (Bio Project Accession No.: **PRJNA1505738**). Following quality filtering and alignment to the *H. pylori* 26695 reference genome (GenBank: AE000511), high-confidence expression values were obtained for 1,564 annotated ORFs.

The original genome sequence of *H. pylori* 26695 reported 1,590 coding sequences (**Tomb 1997**), whereas current genome annotations indicate approximately 1,564 protein-coding genes after exclusion of pseudogenes and non-functional ORFs (**Kanehisa et al. 2025**; **Karp et al. 2019**). In our dataset, approximately 26 ORFs showed no detectable expression and likely corresponded to pseudogenes or transcriptionally inactive loci under given experimental conditions. Therefore, the expression profiles of 1,564 ORFs (Hp0001-Hp1590) were visualized in a genome-wide heatmap **(Fig. 1A)**.

Distinct transcriptional patterns were observed under moderate (pH 5.5) and extreme (pH 2.5) acid stress. Exposure to pH 2.5 produced extensive regions of strongly induced (red) and repressed transcripts (green) across the genome, whereas pH 5.5 elicited comparatively milder and more gradual changes in gene expression. Similar patterns were observed at both 30 min and 4 h, although differences in the magnitude of transcriptional changes were evident between the early (30 min) and prolonged (4 h) exposure periods **(Fig. 1A)** (**Loh et al. 2021**; **Marcus et al. 2018**).

The stacked distribution of $\log_2$ fold-change values further highlighted the differences between moderate and extreme acid stress **(Fig. 1B)**. At pH 2.5 after 30 min, a large proportion of genes exhibited pronounced changes in expression ($\log_2$FC ≥ +2.5 or ≤ −2.5), indicating a robust early transcriptional response. Following 4 h of exposure to pH 2.5, the proportion of highly regulated genes decreased, accompanied by an increase in genes showing moderate expression changes ($\log_2$FC between 0.5 and 1.5). In contrast, under pH 5.5, the majority of transcripts at both time points clustered around $\log_2$FC values between -0.5 and 0.5, indicating relatively limited perturbation of the transcriptome. Collectively,

these observations suggest that nearly half of the *H. pylori* genome (~800 genes) undergoes significant transcriptional changes during severe acid stress.

Temporal changes in gene expression were further examined by scatter plots comparing log_2FC values at 30 min and 4 h under each pH condition **(Fig. 1C, D)**. At pH 2.5, the scatter plot exhibited an asymmetric distribution, with a large cluster of genes above the line of equivalence, indicating higher differential expression at 30 min followed by reduced expression after 4 h. A complementary cluster below the diagonal represented genes showing increased differential expression during prolonged acid exposure. In contrast, the distribution at pH 5.5 was more symmetrical with fewer extreme outliers, reflecting a more consistent transcriptional response over time **(Fig. 1D)** (**Dong et al. 2001**). Overall, these genome-wide analyses demonstrate that *H. pylori* 26695 exhibits a pronounced early transcriptional response under the extreme (pH 2.5) acid stress as compared to moderate (pH 5.5) acid stress where gradual and sustained change has been observed in gene expression.

Acid stress triggers genome-wide and position-independent transcriptional remodelling

To determine whether acid-responsive transcriptional changes were preferentially localized to specific genomic regions. The 1,564 expressed genes were arranged into six consecutive genomic bins (Hp0001-Hp0250, Hp0251-Hp0500, Hp0501-Hp0750, Hp0751-Hp1000, Hp1001-Hp1250, and Hp1251-Hp1590), and the distribution of log_2 fold-change (log_2FC) values within each bin was visualized using box-and-scatter plots **(Fig. S8)**. Genes with log_2FC values between ±0.5 and ±2.5 were considered acid responsive, whereas genes with log_2FC values between −0.5 and 0.5 were considered unchanged.

At pH 2.5 after 30 min, all six genomic bins displayed broadened interquartile ranges compared with the pH 7.4 control, indicating extensive transcriptional changes across the genome **(Fig. S8 A)** (**Loh et al. 2021**). Individual genes with extreme expression values reached approximately ±5 log_2FC, and several bins exhibited a positive shift in median expression values. Similar distributions were observed after 4 h of exposure to pH 2.5, although the spread of extreme responders was slightly reduced **(Fig. S8 B)**. Upregulated and downregulated genes were detected in all six genomic bins at both time points, indicating that transcriptional changes were not restricted to specific genomic segments.

In contrast, exposure to pH 5.5 produced comparatively narrower distributions centred around the zero baseline at both 30 min and 4 h **(Fig. S8 C, D)**. Fewer genes exhibited log_2FC values greater than ±2.5, consistent with a lower magnitude of transcriptional perturbation under moderate acid stress. Similar to pH 2.5, inducible and repressible genes were distributed throughout all genomic bins, with no evidence of preferential clustering within any particular region of the genome.

Collectively, these observations indicate that acid-induced transcriptional remodelling in *H. pylori* 26695 is genome-wide and largely independent of gene position, with responsive genes distributed across the genome rather than concentrated within discrete genomic regions.

Putative TA genes are enriched among acid stress-responsive transcripts of *H. pylori* 26695

The genome-wide and position-independent transcriptional remodelling observed under acid stress prompted us to examine whether specific functional gene groups were preferentially represented among differentially expressed transcripts. To address this, we investigated the expression profiles of the 80 putative toxin-antitoxin (TA) genes previously identified in *H. pylori* 26695 (**Gupta et al. 2022**). Hierarchical clustering of these genes extracted from the RNA-seq dataset revealed distinct expression patterns across the four acid stress conditions **(Fig. 2A)**. A subset of TA loci showed pronounced upregulation under pH 2.5, whereas the response at pH 5.5 was comparatively attenuated. Another cluster displayed transient induction at pH 2.5 after 30 min, followed by reduced expression after 4 h (**Fig. S9)**. In contrast, a small group of genes, including Hp0762 (inner membrane chaperone lipoprotein), Hp0763 (Signal recognition particle receptor- FtsY), Hp0774 (Tyrosine tRNA ligase - tyrS) and Hp0775 (Penta-phosphate guanosine-3'-pyrophosphohydrolase - SpoT), exhibited repression under extreme acid stress.

To investigate the overlap of differentially expressed genes among the four stress conditions, four-way Venn diagrams were constructed for both upregulated and downregulated transcripts **(Fig. 2 B, C)**. Among the 1,564 expressed ORFs, 112, 64, 110 and 98 genes were exclusively upregulated under pH 2.5, 30 min & 4 h; pH 5.5, 30 min &4 h, respectively, whereas only 38 genes were commonly upregulated under all four conditions. Similarly, 99, 84, 127 and 86 genes were uniquely downregulated under the respective stress conditions, with only 32 genes shared among all four conditions. These results indicate that acid-responsive transcriptional changes are largely condition-specific.

A similar analysis performed exclusively on the 80 putative TA genes revealed an even lower degree of overlap among the four stress conditions **(Fig. 2 D, E)**. Most TA genes responded to one or two specific conditions, with only four genes commonly upregulated and a single gene commonly downregulated across all four conditions. These observations indicate that TA genes exhibit distinct expression profiles depending on the severity and duration of acid exposure.

Together, these findings demonstrate that putative TA genes constitute a highly responsive subset of the *H. pylori* transcriptome and display condition-dependent expression patterns under both moderate (pH 2.5) and extreme (pH 2.5) acid stress. The preferential induction of several TA loci at pH 2.5 and their differential expression under pH 5.5 provide transcriptomic evidence that these genes participate in the acid stress response of *H. pylori* 26695.

Genomic organisation and expression profiling of putative toxin-antitoxin genes in *H. pylori* 26695

The enrichment of acid-responsive transcripts among the 80 putative toxin-antitoxin (TA) genes drives a locus-by-locus analysis of their genomic organization and expression patterns. The 48 predicted TA loci identified previously (**Gupta et al. 2022**) were mapped onto the *H. pylori* 26695 genome (NC_000915) and integrated with RNA-seq expression profiles from all four acid stress conditions to generate a genome-wide circular map, and an expression-annotated locus are summarized in **Table 1** and illustrated in **Fig. 3**.

These 48 loci comprised 80 genes organized into 43 operons, of which 39 could be assigned to known Pfam-associated TA families. ParBC represented the largest family (14 loci) (**Chen et al. 2015**), followed by Zeta-Epsilon (5) (**Rocker and Meinhart 2015**), YafQ-DinJ (4) (**Han et al. 2013**; **Han et al. 2011**; **Zhao et al. 2013**), HicAB (3) (**Jørgensen et al. 2009**), Phd-Doc (3) (**Park et al. 2026**), MraZ (2) (**Sprenger et al. 2017**), and SpoIIS (2), whereas HipAB, Fic, SymE1, Hok1, AbiEii1, and NikR1 were represented by single loci (**Dy et al. 2014**; **Harms et al. 2016**; **Kawano 2012**; **Turnbull and Gerdes 2017**; **Van Vliet et al. 2004**) **(Fig. 3, inset)**. Four loci remained unclassified, and five genes were present as orphan toxin or antitoxin components lacking a cognate partner. Both AT→T and T→AT operon orientations were observed throughout the genome, with no strand bias, indicating that the genomic architecture of TA systems in *H. pylori* is organised independently of chromosomal context and that both orientations are equally competent for functional operon activity.

Comparison of expression profiles across the four stress conditions revealed marked condition-dependent regulation of TA genes **(Table 1)**. Overall, the differential expression were more pronounced at pH 2.5 as compared to pH 5.5. Several toxin genes showed more frequent upregulation than their cognate antitoxins under severe acid stress. Members of the Phd-Doc family showed sustained upregulation at both 30 min and 4 h under pH 2.5. Similarly, multiple Zeta-Epsilon loci and AbiEii1 displayed increased expression under severe acid exposure. YafQ-DinJ family members showed strong induction at pH 2.5 after 30 min, whereas SpoIIS loci were transiently induced at 30 min and returned to lower expression levels after 4 h. In contrast, ParBC loci displayed heterogeneous responses, with some members showing moderate induction and others exhibiting little or no change.

The circular genome map further demonstrated that acid-responsive TA loci were distributed throughout the chromosome without obvious clustering **(Fig. 3)**. This pattern was consistent with the genome-wide analysis presented in **Fig. S8** and indicated that acid-responsive TA genes are spatially dispersed across the *H. pylori* genome.

Collectively, **Table 1** and **Figs. 3 and S8** provide a genome-wide overview of the diversity, organization, and stress-responsive expression patterns of putative TA systems in *H. pylori* 26695. Based on these expression profiles, 21 representative TA loci encompassing the major families were selected for operon validation (data unpublished) and subsequent qRT-PCR analysis.

RNA-seq validation using functionally characterised control genes.

Before proceeding with further analyses, the reliability of the RNA-seq dataset was evaluated by comparing expression profiles with qRT-PCR measurements (**de Brito et al. 2024**; **Tubau-Juni et al. 2020**). Seven functionally characterized genes of *H. pylori* 26695 were selected as controls, representing urease-dependent acid adaptation (ureA and ureI (**Ansari and Yamaoka 2017**; **Scott et al. 2002**), housekeeping functions (gyrA and rpoB) (**Austin and Maier 2013**; **Elbaiomy et al. 2025**; **Wen et al. 2003**), motility (flaA) (**De la Cruz et al. 2017**; **Spohn and Scarlato 1999**; **Wen et al. 2003**), and urease-independent nitrogen metabolism (aimE and rocF) (**Jones et al. 2018**; **Pflock et al. 2006**; **Wen et al. 2003**). The qRT-PCR analysis was performed in duplicate, and expression values i.e Ct value were

normalized using the geometric mean of 16S and 23S rRNA Ct values (**Vandesompele et al. 2002**). Statistical analyses were performed using Origin 2024 (Delhi University Computer Centre license).

Because no urea was added to the acid stress medium, urease-mediated buffering was absent (**Sachs et al. 2001**). Accordingly, both ureA and ureI were downregulated under all four acid stress conditions in both datasets. At pH 2.5 after 4 h, ureA and ureI exhibited log_2FC, -1.33 and -1.49, respectively. Similarly, the housekeeping genes gyrA and rpoB were consistently repressed under all conditions, with rpoB showing the strongest reduction at pH 2.5 after 4 h, reaching log_2FC, -3.847 and -4.157 in RNA-seq and qRT-PCR datasets, respectively. In contrast, flaA was induced under pH 2.5 after 30 min, with log_2FC, +2.764 and +3.096 obtained by RNA-seq and qRT-PCR, respectively. The nitrogen metabolism-associated genes aimE and rocF were upregulated under severe acid stress in both datasets; at pH 2.5 after 30 min, aimE reached log_2FC +1.5 and +2.6693 in RNA-seq and qRT-PCR, respectively, and rocF reached log_2FC +3.2475 and +3.0134 in RNA-seq and qRT-PCR, respectively.

Overall, RNA-seq and qRT-PCR exhibited highly consistent expression patterns **(Fig. 4)**. Genes that were upregulated or downregulated in the RNA-seq analysis showed corresponding trends in the qRT-PCR data, suggesting the consistency of the results. Although minor differences in absolute log_2FC were observed, likely due to differences in dynamic range and normalization procedures, the relative expression patterns remained highly similar. Correlation analysis demonstrated a strong positive relationship between the two approaches ($R = 0.954$, $p < 0.001$), supporting the reliability of the RNA-seq dataset and providing a robust basis for subsequent analyses of toxin-antitoxin genes and operons.

qRT-PCR validation of individual toxin-antitoxin gene expression profiles.

Following validation of the control genes, we extended the analysis to selected toxin-antitoxin (TA) loci identified in our previous genome-wide study (**Gupta et al. 2022**). 21 putative TA operons comprising 40 individual toxin (T) and antitoxin (AT) genes were selected for expression analysis. RNA-seq-derived log_2FC values were compared with qRT-PCR expression under four acid stress conditions compared to control (pH 7.4) **(Fig. 5)**. The overall distribution of individual gene expression profiles obtained by both methods is shown in the scatter plots **(Fig. 5A, B)**.

Gene-wise comparisons were further visualized using bar plots **(Fig. 5C, D)**. The selected genes included members of the Zeta-Epsilon, YafQ-DinJ, VapBC, Phd-Doc, AbiEii and other predicted TA families. The direction of expression changes was highly consistent between RNA-seq and qRT-PCR. Genes that were upregulated or downregulated in the RNA-seq analysis exhibited the same trend in qRT-PCR, whereas only a few genes within the unchanged range (log_2FC between -0.5 and +0.5) showed a minor difference.

The strongest induction was observed under severe acid stress (pH 2.5, 30 min). Hp0993, Hp0994 and Hp1497 displayed the highest positive log_2FC values, exceeding +4 in both RNA-seq and qRT-PCR datasets. In general, expression levels induced at 30 min decreased at 4 h, although most remained above the baseline. In contrast, expression changes at pH 5.5 were comparatively moderate and remained closer to the zero baseline in both datasets **(Fig. 5A, B)**.

Using a threshold of $\log_2$ FC ≥ 0.5, 10 toxin genes and 10 antitoxin genes were upregulated at pH 2.5 after 30 min, whereas 13 toxin genes and 11 antitoxin genes were upregulated after 4 h. Under mild acid stress (pH 5.5), 7 toxin genes and 7 antitoxin genes were upregulated after 30 min, while 4 toxin genes and 10 antitoxin genes showed increased expression after 4 h. In comparison, downregulated genes represented less than 17% of the selected TA genes across all conditions **(Fig. 5).**

To further evaluate the agreement between both techniques, Pearson correlation analysis was performed for each condition **(Fig. 6A-D)**. Strong positive correlations were obtained for pH 2.5 after 30 min (r = 0.9103), pH 2.5 after 4 h (r = 0.9565), pH 5.5 after 30 min (r = 0.9034), and pH 5.5 after 4 h (r = 0.9453), with all correlations being statistically significant ($p < 0.0001$; n = 40). When all four conditions were pooled (n = 160), the overall correlation coefficient was r = 0.9280 ($p < 0.0001$) **(Fig. 6E)**. Among individual conditions, pH 2.5 after 4 h exhibited the highest agreement between RNA-seq and qRT-PCR datasets **(Fig. 6F)**.

Comparison of toxin and antitoxin components also revealed asymmetric expression patterns in several TA loci. In the Hp0892-Hp0893 and Hp0894-Hp0895 systems, previously characterized in *H. pylori* (**Han et al. 2013**; **Han et al. 2011**), as well as in the Hp0993-Hp0994 locus, the antitoxin component displayed greater fold changes than the corresponding toxin gene under severe acid stress. These observations obtained independently by qRT-PCR further support the transcriptional dynamics revealed by RNA-seq and confirm that acid-responsive regulation of TA genes represents a reproducible and biologically relevant feature of *H. pylori* 26695.

qRT-PCR expression analysis of selected toxin-antitoxin operons

Having validated the RNA-seq dataset using control genes **(Fig. 4)** and individual toxin and antitoxin genes **(Fig. 5 and 6)**, we next examined expression at the operon level by calculating $\log_2$FC values for 21 selected TA operons. Operon-level expression values were normalized using the geometric mean of 16S and 23S rRNA Ct values as the reference baseline **(Fig. 7A)**. Heatmap visualization together with scatter and bar plots **(Fig. 7A- C),** revealed a pronounced condition-dependent pattern of operon expression.

Most TA operons (18 of 21) were upregulated under severe acid stress at pH 2.5, both after 30 min and 4 h. The strongest induction at pH 2.5 after 30 min was observed for Hok1, ParBC4, SymE1, YafQ1, Fic1 and NikR1, each exhibiting $\log_2$FC values exceeding +2.5 **(Fig. 7C)**. In contrast, MraZ2 displayed a distinct expression profile characterized by marked downregulation at pH 2.5 after 30 min and only weak transient induction at pH 5.5 after 30 min. Likewise, Zeta2 showed partial downregulation at pH 2.5 and moderate induction at pH 5.5, suggesting differential regulation compared with the majority of the operons.

Expression changes under mild acid stress (pH 5.5) were generally smaller, with most operons exhibiting $\log_2$Fc values close to zero or only slight induction **(Fig. 7 A, C)**. Among the different TA families, Phd-Doc1, Phd-Doc2 and Phd-Doc3 maintained elevated expression at both pH 2.5 time points with

comparatively limited attenuation after 4 h. Overall, the operon-level qRT-PCR data also confirmed that acid stress induces widespread but differential transcriptional responses among TA systems in *H. pylori* 26695.

To highlight the temporal dynamics of these responses, qRT-PCR-validated genes and operons were classified according the increased or decreased expression profile in between 30 min and 4 h under each pH condition. Paired violin-slope plots were generated to visualize the trajectories of log_2FC values **(Fig. S10)**. At pH 2.5, 23 genes and 10 operons exhibited increased expression over time, whereas 17 genes and 11 operons showed reduced expression. In contrast, fewer changes were observed under pH 5.5. These findings indicate that acid-responsive regulation of TA systems involves both activation and attenuation of distinct loci during prolonged acid exposure rather than a uniform transcriptional response.

Network-based analysis of toxin-antitoxin regulatory relationships under acid stress.

Having validated the expression profiles of individual TA genes and operons **(Fig. 5 – 7, S9-S10)**, we next sought to visualize their relationships across the four acid stress conditions. An integrated network was constructed using qRT-PCR-derived log_2FC values to represent the interactions between individual TA genes, their corresponding operons, and the different stress conditions **(Fig. 8)**. In this network, circular nodes represent TA genes, octagonal nodes represent TA operons, and square nodes correspond to the four acid stress conditions. Node colour reflects the magnitude and direction of expression changes, while edge weights represent the relative strength of transcriptional responses.

The overall network displayed a clear bipartite organisation, with activated and deactivated expression modules occupying distinct regions. The right side of the network was dominated by highly induced genes and operons, including Hp0993, Hp0994, Hp0895, AbiEii1, SymE1, PhdDoc2, YafQ2, Hok1 and Hp1338. These nodes showed dense connections with the activation condition nodes, particularly under severe acid stress at pH 2.5, consistent with the strong induction patterns observed previously **(Fig. 5 – 7)**. In contrast, the left side of the network contained predominantly repressed nodes, including MraZ2, gyrA, rpoB, ureA, ureI, flaA, Hp0240, Hp0593 and Hp0763, which were associated with the deactivation condition nodes. This spatial separation highlights that acid stress induces coordinated activation and repression of distinct groups of genes rather than causing a uniform transcriptional perturbation.

Several nodes occupied central positions within the network and were connected to both activated and deactivated modules. Such connectivity reflected the biphasic expression patterns observed in the temporal analyses **(Figs. 7 and S10)**, where some genes and operons exhibited different responses depending on pH and exposure time. Among the operons, ParBC4, PhdDoc1 and NikR1 showed extensive connectivity within the activation subnetwork and formed tightly associated clusters under pH 2.5 conditions. Their prominent positions suggest that these operons may participate in broader stress-responsive transcriptional programs during severe acid exposure.

Overall, the network architecture provides a systems-level representation of the acid-responsive TA landscape in *H. pylori* 26695 **(Fig. 8)**. The coexistence of activated and repressed modules and their extensive interconnections indicate that TA systems are integrated components of the bacterial stress response and may contribute collectively to the adaptive strategies that enable survival under harsh acidic conditions.

Filtered expression profiles of protease and acid-resistance genes under acid stress

Beyond the transcriptional profiling of toxin-antitoxin (TA) systems, the genome-wide RNA-seq dataset also contained several functionally important groups of genes, including proteases and acid-resistance (AR) associated genes **(Fig. 9)**. To place the TA-mediated responses into a broader physiological context, we examined the expression dynamics of these functional categories under the four acid stress conditions. Sankey flow diagrams were used to visualize the proportions of upregulated (red), unchanged (grey), and downregulated (green) genes within each group **(Fig. 9A, B)**.

Among the 13 protease-encoding loci (**Karp et al. 2019**; **Löwer et al. 2008**; **Posselt, Crabtree and Wessler 2017**; **Tomb 1997**; **Wessler and Posselt 2024**), the strongest response was observed under severe acid stress at pH 2.5 for 30 min, where 62% of the genes were downregulated, whereas only 23% were upregulated **(Fig. 9A) (Fig. S.13)**. At pH 2.5 for 4 h, repression remained predominant. In contrast, mild acidification at pH 5.5 produced comparatively smaller changes, with most protease genes remaining unchanged, indicating that moderate acidity exerts only limited effects on the proteolytic machinery.

A contrasting pattern was observed for the 10 acid-resistance (AR) associated genes (**Häuser et al. 2014**; **Karp et al. 2019**; **Rain et al. 2001**; **Tomb 1997**; **Tran et al. 2004**; **Vallese et al. 2015**). At both pH 2.5 (30 min) and pH 5.5 (30 min), approximately half of the AR genes were upregulated **(Fig. 9B)**, consistent with activation of the canonical acid-response machinery. These genes included the urea channel UreI (Hp0071), glutamate dehydrogenase GdhA (Hp0380), aliphatic amidase AimE (Hp0294), L-asparaginase II ansB (Hp0723) and the response regulator Hp1021 (**Donczew et al. 2015**; **Miller Erica and Maier Robert 2014**; **Scott et al. 2002**; **Skouloubris et al. 2001**; **Smith et al. 2007**; **Yang et al. 2022**; **Zanotti and Cendron 2014**). However, following prolonged exposure to severe acid stress, i.e. pH 2.5 (4 h), the proportion of upregulated acid-resistance (AR) associated genes decreased to 40%, whereas approximately 50% of the genes became downregulated, indicating a temporal shift in the acid-response programme **(Fig. S.14)**.

Collectively, these expression patterns indicate that *H. pylori* 26695 mounts a graded and functionally stratified response to acid stress, with protease-associated genes and classical acid-resistance determinants exhibiting distinct transcriptional behaviours depending on both pH severity and duration of exposure.

Discussion

The present study provides the first genome-wide transcriptomic characterization of putative toxin-antitoxin (TA) systems in *H. pylori* 26695 under acid stress. We examined TA gene expression at the gene, operon, and network levels. Together, our findings suggest that *H. pylori* employ its TA repertoire as part of a temporally coordinated and severity-dependent acid-stress response.

RNA-Seq showed that nearly half of the *H. pylori* genome altered its expression under severe acid stress (pH 2.5). This response was much broader than previously reported studies that mainly focused on selected acid-responsive genes (Ang et al. 2001; Loh et al. 2021; Merrell et al. 2003). The scatter plots showed a strong response at 30 min followed by partial attenuation at 4 h, suggesting a two-phase transcriptional programme. Similar biphasic responses have been described in other stress-adapted bacteria and are considered a common strategy for survival under hostile conditions (Choudhary, Foster and Uphoff 2024; Cortes et al. 2017; **Merchel et al. 2020**; Yuan et al. 2026). Such responses allow an initial emergency phase to be replaced by a metabolically sustainable adaptive state (Sharma et al. 2025). In addition, the absence of positional bias across the genome indicates that acid-induced transcriptional changes are primarily controlled through trans-acting regulatory mechanisms rather than local genome organization (Song et al. 2021; Sun et al. 2020).

One of the most important findings of this study was the enrichment of putative TA genes among acid-responsive transcripts. TA systems are recognized as stress-responsive elements in many bacteria, particularly in *E. coli*, where they contribute to growth arrest and persistence *E. coli (*Fiedoruk et al. 2015; Yamaguchi and Inouye 2011*)*. In *H. pylori*, however, only four type II TA systems have been experimentally characterized to date (Han et al. 2013; Han et al. 2011). Their genome-wide response to acid stress has not been explored previously. Hierarchical clustering of 80 putative TA genes revealed distinct co-expression clusters, with most genes strongly induced at pH 2.5. The Venn analysis further showed that individual loci responded differently under different conditions. Thus, TA genes do not behave as a single co-regulated block. Instead, they appear to form a modular and condition-specific regulatory network. Such flexibility may allow *H. pylori* to adapt to the heterogeneous microenvironments encountered within the gastric mucosa (Marcus et al. 2018).

Analysis of the 48 putative TA loci revealed substantial differences among TA families. The PhdDoc family showed sustained induction during prolonged exposure to pH 2.5. PhdDoc toxins are sequence-specific endoribonucleases, and prolonged activation of this family may contribute to translational slowing and reduced metabolic activity, characteristics frequently associated with persistence (Park et al. 2026). Members of the YafQ-DinJ family were strongly induced during the early phase of severe acid stress. YafQ toxins are mRNA interferases and are known to participate in stress adaptation and persistence (Han et al. 2013; Han et al. 2011; Hu et al. 2024). Similarly, HipAB1 was induced under severe acid stress. HipA-family toxins are ATP-dependent serine kinases and have been implicated in persister-cell formation in several bacterial pathogens (Lewis and Hansen 2012; Zhao et al. 2013). Our observations suggest that these systems may also participate in acid adaptation in *H. pylori*.

Another interesting observation was the asymmetric expression between toxin and antitoxin genes. Under severe acid stress, toxin transcripts were frequently more abundant than their corresponding antitoxin transcripts. Although transcript abundance does not necessarily reflect protein levels, this pattern suggests altered toxin-antitoxin stoichiometry under acidic conditions. Such imbalances have been proposed to favour toxin activity and growth attenuation in other bacterial systems *E. coli (*Fiedoruk et al. 2015; Yamaguchi and Inouye 2011*)*. Therefore, selective activation of toxin components may contribute to metabolic slowing during prolonged acid stress.

The qRT-PCR experiments strongly supported the RNA-seq data. Validation using well-characterized control genes showed excellent agreement between both approaches. Similar patterns were also observed for the 40 individual TA genes. No major directional differences were detected. These findings confirm that the RNA-seq matrix accurately reflects the transcriptional behaviour of TA genes under acid stress and support the biological relevance of the observed changes.

Operon-level analysis further demonstrated that TA induction depends on acid severity. Most operons were strongly induced at pH 2.5 but showed weaker responses at pH 5.5. This finding suggests that the TA response of *H. pylori* is quantitatively tuned to the degree of acid stress rather than behaving as an all-or-none switch. Severe acidification triggered stronger transcriptional activation, whereas milder acid stress produced a more moderate response. Among the operons, MraZ2 displayed a unique pattern. It was repressed at pH 2.5 but transiently induced at pH 5.5. MraZ proteins act as transcriptional regulators of cell division genes in other bacteria (**Eraso et al. 2014**; White et al. 2022). Therefore, MraZ2 may contribute to selective growth resumption under moderate acid conditions.

The temporal analyses and network modelling provided a systems-level view of TA regulation. Activated and deactivated modules occupied distinct regions of the network, indicating that the response is highly organized rather than random. Several operons, including ParBC4, PhdDoc1 and NikR1, occupied central positions within the activation network. Their high connectivity suggests that these operons may act as regulatory hubs that integrate stress signals with downstream adaptive responses. Similar network-based architectures have been reported in stress-responsive regulatory circuits of bacterial pathogenesis (Choudhary et al. 2024; Cortes et al. 2017).

Taken together, our findings show that the TA landscape of *H. pylori* is transcriptionally active, functionally diverse, and highly responsive to acid stress. We propose that acid exposure triggers genome-wide transcriptional remodelling that activates both classical acid-resistance pathways and selected TA systems. Prolonged severe acidification may favour a low-energy physiological state compatible with survival in the gastric niche. Although functional validation is still required, our results suggest that TA systems represent previously underappreciated components of acid adaptation and may contribute to the remarkable persistence of *H. pylori* within the human stomach. Such systems may also represent attractive targets for anti-persistence therapeutic strategies (Lewis and Hansen 2012; Yamaguchi and Inouye 2011).

Conclusion

This study provides the first genome-wide analysis of acid stress-responsive toxin-antitoxin (TA) systems in *H. pylori* 26695. Acid stress caused extensive transcriptional changes across the genome. Extreme acid stress (pH 2.5) produced stronger responses than moderate acid stress (pH 5.5). These changes were distributed throughout the genome and were not restricted to specific genomic regions.

Putative TA genes were highly enriched among acid-responsive transcripts. Different TA loci and operons showed distinct pH and time-dependent expression patterns. Some families displayed transient induction, whereas others remained active during prolonged stress. This indicates that TA systems are regulated in a selective and dynamic manner.

The RNA-seq results were supported by qRT-PCR analysis of control genes and individual TA genes. Strong agreement between the two approaches confirmed the reliability of the transcriptomic data. Network analysis further showed that TA genes and operons form interconnected regulatory modules rather than acting as isolated genetic elements.

Together, these findings suggest that TA systems are an active part of the acid stress response of *H. pylori*. Their selective activation under extreme acid conditions points to a possible role in growth modulation and persistence within the gastric environment. This work provides a framework for future functional studies aimed at understanding the role of individual TA systems and evaluating their potential as targets for anti-persistence therapeutic strategies.

Declarations

Acknowledgment: The authors are grateful to Prof. Suman Kumar Dhar for providing access to the culture facility at the Special Centre for Molecular Medicine (SCMM), Jawaharlal Nehru University (JNU), New Delhi, for conducting the *Helicobacter pylori* 26695 culture. The authors also thank Prof. Vijay Kumar Prajapati, Department of Biochemistry, University of Delhi South Campus, New Delhi, for providing access to the qRT-PCR facility used in this study. The authors acknowledges the University of Delhi Computer Centre (DUCC) for providing access to the academic license of OriginPro 2024 and other institutional software resources used in this study.

Conflict of Interest: There are no competing interests to declare from authors.

Ethical Approval: Not applicable.

Funding: This work was supported by the Department of Health Research (DHR), Ministry of Health and Family Welfare, Government of India, under the HRD Scheme (File No. R.12013/49/2024-HR) awarded to NG. This work was also supported by an ICMR Adhoc Research Grant (Grant No. 2020-3613/CMB/Adhoc-BMS) awarded to V.K.V. D.K.B. and M.Y. got fellowship support from the University Grants Commission (UGC), Government of India, and the Department of Biotechnology (DBT), Government of India, respectively.

Author's Contribution: Conceptualization: D.K.B., N.G., and V.K.V..; Data curation: D.K.B. and N.G.; Formal analysis: D.K.B. and N.G.; Investigation: D.K.B., N.G., and V.K.V; Methodology: D.K.B., M.Y. and N.G.; Project administration: D.K.B., N.G., and V.K.V; Resources: N.G., and V.K.V; Software: D.K.B., N.G., and V.K.V; Supervision: N.G., and V.K.V; Validation: D.K.B., M.Y., N.G., and V.K.V; Visualization: D.K.B., M.Y., N.G., and V.K.V; Writing-original draft: D.K.B., and N.G.; Writing-review & editing: D.K.B., M.Y., N.G., and V.K.V. All authors have read and agreed to this version of the manuscript.

Availability of RNASeq raw data: The datasets generated and analysed during the current study are available from the corresponding author on reasonable request. Raw RNA-seq sequencing data generated in this study are available in the NCBI Sequence Read Archive (SRA) under BioProject accession **PRJNA1505738**.

References

1. Akbari A, Noorbakhsh Varnosfaderani SM, Haeri MS, Fathi Z, Aziziyan F, Yousefi Rad A, Zalpoor H, Nabi-Afjadi M, Malekzadegan Y (2024) Autophagy induced by *Helicobacter pylori* infection can lead to gastric cancer dormancy, metastasis, and recurrence: new insights. Human Cell 37(1):139-153
2. Andersson R, Gebhard C, Miguel-Escalada I, Hoof I, Bornholdt J, Boyd M, Chen Y, Zhao X, Andrews S (2010) FastQC: A quality control tool for high throughput sequence data. Version 011 2
3. Ang S, Lee CZ, Peck K, Sindici M, Matrubutham U, Gleeson MA, Wang JT (2001) Acid-induced gene expression in *Helicobacter pylori*: study in genomic scale by microarray. Infect Immun 69(3):1679-86
4. Ansari S, Yamaoka Y (2017) Survival of *Helicobacter pylori* in gastric acidic territory. Helicobacter 22(4):e12386
5. Austin CM, Maier RJ (2013) Aconitase-mediated posttranscriptional regulation of *Helicobacter pylori* peptidoglycan deacetylase. Journal of bacteriology 195(23):5316-5322
6. Bauer B, Meyer TF (2011) The Human Gastric Pathogen *Helicobacter pylori* and Its Association with Gastric Cancer and Ulcer Disease. Ulcers 2011(1):340157
7. Blanchard TG, Nedrud JG (2006) Laboratory maintenance of Helicobacter species. Curr Protoc Microbiol Chapter 8:Unit8B.1
8. Boampong K, Smith SL, Delahay RM (2020) Rapid growth inhibitory activity of a YafQ-family endonuclease toxin of the *Helicobacter pylori* tfs4 integrative and conjugative element. Scientific Reports 10(1):18171
9. Chen B-W, Lin M-H, Chu C-H, Hsu C-E, Sun Y-J (2015) Insights into ParB spreading from the complex structure of Spo0J and parS. Proc Natl Acad Sci U S A 112(21):6613-6618
10. Chen S (2023) Ultrafast one-pass FASTQ data preprocessing, quality control, and deduplication using fastp. iMeta 2(2):e107
11. Choudhary D, Foster K, Uphoff S (2024) The master regulator OxyR orchestrates bacterial oxidative stress response genes in space and time. Cell systems 15:1033-1045

12. Cortes T, Schubert O, Banaei-Esfahani A, Collins B, Aebersold R, Young D (2017) Delayed effects of transcriptional responses in *Mycobacterium tuberculosis* exposed to nitric oxide suggest other mechanisms involved in survival. Scientific Reports 7
13. Cover Timothy L (2016) *Helicobacter pylori* Diversity and Gastric Cancer Risk. mBio 7(1):10.1128/mbio.01869-15
14. de Brito MWD, de Carvalho SS, Mota M, Mesquita RD (2024) RNA-seq validation: software for selection of reference and variable candidate genes for RT-qPCR. BMC Genomics 25(1):697
15. De la Cruz MA, Ares MA, Von Bargen K, Panunzi LG, Martínez-Cruz J, Valdez-Salazar HA, Jiménez-Galicia C, Torres J (2017) Gene expression profiling of transcription factors of *Helicobacter pylori* under different environmental conditions. Frontiers in microbiology 8:615
16. Donczew R, Makowski Ł, Jaworski P, Bezulska M, Nowaczyk M, Zakrzewska-Czerwińska J, Zawilak-Pawlik A (2015) The atypical response regulator HP1021 controls formation of the *Helicobacter pylori* replication initiation complex. Molecular Microbiology 95(2):297-312
17. Dong Q, Hyde D, Herra C, Kean C, Murphy P, O'Morain CA, Buckley M (2001) Identification of genes regulated by prolonged acid exposure in *Helicobacter pylori*. FEMS Microbiology Letters 196(2):245-249
18. Dy RL, Przybilski R, Semeijn K, Salmond GP, Fineran PC (2014) A widespread bacteriophage abortive infection system functions through a Type IV toxin-antitoxin mechanism. Nucleic Acids Res 42(7):4590-605
19. El Mortaji L, Tejada-Arranz A, Rifflet A, Boneca IG, Pehau-Arnaudet G, Radicella JP, Marsin S, De Reuse H (2020) A peptide of a type I toxin–antitoxin system induces *Helicobacter pylori* morphological transformation from spiral shape to coccoids. Proceedings of the National Academy of Sciences 117(49):31398-31409
20. Elbaiomy RG, Luo X, Guo R, Deng S, Du M, El-Sappah AH, Bakeer M, Azzam MM, Elolimy AA, Madkour M, Li Z, Zhang Z (2025) Antibiotic resistance in *Helicobacter pylori*: a genetic and physiological perspective. Gut Pathogens 17(1):35
21. Eraso Jesus M, Markillie Lye M, Mitchell Hugh D, Taylor Ronald C, Orr G, Margolin W (2014) The Highly Conserved MraZ Protein Is a Transcriptional Regulator in *Escherichia coli*. Journal of Bacteriology 196(11):2053-2066
22. Fiedoruk K, Daniluk T, Swiecicka I, Sciepuk M, Leszczynska K (2015) Type II toxin–antitoxin systems are unevenly distributed among *Escherichia coli* phylogroups. Microbiology 161(1):158-167
23. Green MR, Sambrook J (2019) Removing DNA Contamination from RNA Samples by Treatment with RNase-Free DNase I. Cold Spring Harb Protoc 2019(10)
24. Gupta N, Behera DK, Prajapati VK, Verma VK (2022) A comprehensive approach to discover Toxin-Antitoxin systems from human pathogen *Helicobacter pylori*: A poison and its antidote encapsulated in the genome. Life Sci 288:120149
25. Han KD, Ahn DH, Lee SA, Min YH, Kwon AR, Ahn HC, Lee BJ (2013) Identification of chromosomal HP0892-HP0893 toxin-antitoxin proteins in *Helicobacter pylori* and structural elucidation of their

protein-protein interaction. Journal of Biological Chemistry 288(8):6004-6013

26. Han KD, Matsuura A, Ahn HC, Kwon AR, Min YH, Park HJ, Won HS, Park SJ, Kim DY, Lee BJ (2011) Functional identification of toxin-antitoxin molecules from *Helicobacter pylori* 26695 and structural elucidation of the molecular interactions. Journal of Biological Chemistry 286(6):4842-4853
27. Harms A, Stanger FV, Dehio C (2016) Biological Diversity and Molecular Plasticity of FIC Domain Proteins. Annual Review of Microbiology 70(Volume 70, 2016):341-360
28. Häuser R, Ceol A, Rajagopala SV, Mosca R, Siszler G, Wermke N, Sikorski P, Schwarz F, Schick M, Wuchty S, Aloy P, Uetz P (2014) A second-generation protein-protein interaction network of *Helicobacter pylori*. Mol Cell Proteomics 13(5):1318-29
29. Hu W, Zhai Zhi Y, Huang Zhao Y, Chen Ze M, Zhou P, Li Xia X, Yang Gen H, Bao Chong J, You Li J, Cui Xiao B, Xia Gui L, Ou Yang Mei P, Zhang L, Wu William Ka K, Li Long F, Zhang Yu X, Xiao Zhan G, Gong W (2024) Dual RNA sequencing of *Helicobacter pylori* and host cell transcriptomes reveals ontologically distinct host-pathogen interaction. mSystems 9(4):e00206-24
30. IARC (2012) Biological agents. IARC Monogr Eval Carcinog Risks Hum 100(Pt B):1-441
31. Jones MD, Li Y, Zamble DB (2018) Acid-responsive activity of the *Helicobacter pylori* metalloregulator NikR. Proceedings of the National Academy of Sciences 115(36):8966-8971
32. Jørgensen MG, Pandey DP, Jaskolska M, Gerdes KJJob (2009) HicA of *Escherichia coli* defines a novel family of translation-independent mRNA interferases in bacteria and archaea. 191(4):1191-1199
33. Jurėnas D, Fraikin N, Goormaghtigh F, Van Melderen L (2022) Biology and evolution of bacterial toxin–antitoxin systems. Nature Reviews Microbiology 20(6):335-350
34. Kanehisa M, Furumichi M, Sato Y, Matsuura Y, Ishiguro-Watanabe M (2025) KEGG: biological systems database as a model of the real world. Nucleic Acids Research 53(D1):D672-D677
35. Karp PD, Billington R, Caspi R, Fulcher CA, Latendresse M, Kothari A, Keseler IM, Krummenacker M, Midford PE, Ong Q, Ong WK, Paley SM, Subhraveti P (2019) The BioCyc collection of microbial genomes and metabolic pathways. Briefings in Bioinformatics 20(4):1085-1093
36. Kawano MJRb (2012) Divergently overlapping cis-encoded antisense RNA regulating toxin-antitoxin systems from E. coli: hok/sok, ldr/rdl, symE/symR. 9(12):1520-1527
37. Kim SM, Rahaman MI, Bang CS, Lee S, Kim HW, Kim SW, Ahn JY, Jung HY, Kim YH, Gong EJ (2025) Optimal liquid culture media for *Helicobacter pylori*: Strain-specific growth in different broth formulations. World J Gastroenterol 31(43):111876
38. Langmead B, Salzberg SL (2012) Fast gapped-read alignment with Bowtie 2. Nature Methods 9(4):357-359
39. Lewis K, Hansen S (2012) Type II toxin-antitoxin loci, hipBA and persisters Prokaryotic Toxin-Antitoxins. Springer, pp 189-203
40. Loh JT, Shum MV, Jossart SDR, Campbell AM, Sawhney N, McDonald WH, Scholz MB, McClain MS, Forsyth MH, Cover TL (2021) Delineation of the pH-Responsive Regulon Controlled by the

Helicobacter pylori ArsRS Two-Component System. Infect Immun 89(4)

41. Löwer M, Weydig C, Metzler D, Reuter A, Starzinski-Powitz A, Wessler S, Schneider G (2008) Prediction of Extracellular Proteases of the Human Pathogen *Helicobacter pylori* Reveals Proteolytic Activity of the Hp1018/19 Protein HtrA. PLOS ONE 3(10):e3510
42. Marcus EA, Sachs G, Scott DR (2018) Acid-regulated gene expression of *Helicobacter pylori*: Insight into acid protection and gastric colonization. Helicobacter 23(3):e12490
43. Merchel Piovesan Pereira B, Wang X, Tagkopoulos I (2020) Short- and Long-Term Transcriptomic Responses of *Escherichia coli* to Biocides: a Systems Analysis. Applied and Environmental Microbiology 86(14):e00708-20
44. Merrell D, Goodrich M, Otto G, Tompkins L, Falkow S (2003) pH-Regulated Gene Expression of the Gastric Pathogen *Helicobacter pylori*. Infection and Immunity 71:3529-3539
45. Miller Erica F, Maier Robert J (2014) Ammonium Metabolism Enzymes Aid *Helicobacter pylori* Acid Resistance. Journal of Bacteriology 196(17):3074-3081
46. Page R, Peti WJNcb (2016) Toxin-antitoxin systems in bacterial growth arrest and persistence. 12(4):208-214
47. Pandey DP, Gerdes K (2005) Toxin-antitoxin loci are highly abundant in free-living but lost from host-associated prokaryotes. Nucleic Acids Res 33(3):966-76
48. Park JY, Kim M, Lim B, Kim HJ (2026) Toxin dimerization and a distinct DNA-binding architecture define chromosomal Phd-Doc regulation. Nucleic Acids Research 54(6):gkag280
49. Pflock M, Finsterer N, Joseph B, Mollenkopf H, Meyer TF, Beier D (2006) Characterization of the ArsRS regulon of *Helicobacter pylori*, involved in acid adaptation. Journal of bacteriology 188(10):3449-3462
50. Posselt G, Crabtree JE, Wessler S (2017) Proteolysis in *Helicobacter pylori*-induced gastric cancer. Toxins 9(4):134
51. Rain JC, Selig L, De Reuse H, Battaglia V, Reverdy C, Simon S, Lenzen G, Petel F, Wojcik J, Schächter V, Chemama Y, Labigne A, Legrain P (2001) The protein-protein interaction map of *Helicobacter pylori*. Nature 409(6817):211-5
52. Reshetnyak VI, Reshetnyak TM (2017) Significance of dormant forms of *Helicobacter pylori* in ulcerogenesis. World J Gastroenterol 23(27):4867-4878
53. Richards CL, Buchholz BJ, Ford TE, Broadaway SC, Pyle BH, Camper AK (2011) Optimizing the growth of stressed *Helicobacter pylori*. J Microbiol Methods 84(2):174-82
54. Robinson MD, McCarthy DJ, Smyth GK (2010) edgeR: a Bioconductor package for differential expression analysis of digital gene expression data. Bioinformatics 26(1):139-140
55. Rocker A, Meinhart A (2015) A cis-acting antitoxin domain within the chromosomal toxin–antitoxin module EzeT of *Escherichia coli* quenches toxin activity. Molecular Microbiology 97(3):589-604
56. Sachs G, Scott DR, Weeks DL, Rektorscheck M, Melchers K (2001) Regulation of urease for acid habitation. *Helicobacter pylori*: physiology and genetics:277-283

57. Scott DR, Marcus EA, Weeks DL, Sachs G (2002) Mechanisms of acid resistance due to the urease system of *Helicobacter pylori*. Gastroenterology 123(1):187-195
58. Sharma A, Nitharwal RG, Singh B, Dar A, Dasgupta S, Dhar SK (2009) *Helicobacter pylori* single-stranded DNA binding protein – functional characterization and modulation of H. pylori DnaB helicase activity. The FEBS Journal 276(2):519-531
59. Sharma A, Tayal S, Bhatnagar S (2025) Analysis of stress response in multiple bacterial pathogens using a network biology approach. Scientific Reports 15
60. Sharma CM, Hoffmann S, Darfeuille F, Reignier J, Findeiß S, Sittka A, Chabas S, Reiche K, Hackermüller J, Reinhardt R, Stadler PF, Vogel J (2010) The primary transcriptome of the major human pathogen *Helicobacter pylori*. Nature 464(7286):250-255
61. Skouloubris S, Labigne A, De Reuse H (2001) The AmiE aliphatic amidase and AmiF formamidase of *Helicobacter pylori*: natural evolution of two enzyme paralogues. Molecular microbiology 40(3):596-609
62. Smith TG, Lim JM, Weinberg MV, Wells L, Hoover TR (2007) Direct analysis of the extracellular proteome from two strains of *Helicobacter pylori*. Proteomics 7(13):2240-2245
63. Song Z-T, Liu J-X, Han J-J (2021) Chromatin remodeling factors regulate environmental stress responses in plants. Journal of integrative plant biology
64. Spohn G, Scarlato V (1999) Motility of *Helicobacter pylori* Is Coordinately Regulated by the Transcriptional Activator FlgR, an NtrC Homolog. Journal of Bacteriology 181(2):593-599
65. Sprenger H, Kienesberger S, Pertschy B, Pöltl L, Konrad B, Bhutada P, Vorkapic D, Atzmüller D, Feist F, Högenauer C (2017) Fic proteins of *Campylobacter fetus* subsp. venerealis form a network of functional toxin–antitoxin systems. Frontiers in Microbiology 8:1965
66. Sun L, Jing Y, Liu X, Li Q, Xue Z, Cheng Z, Wang D, He H, Qian W (2020) Heat stress-induced transposon activation correlates with 3D chromatin organization rearrangement in Arabidopsis. Nature Communications 11
67. Tomb JF (1997) The complete genome sequence of the gastric pathogen *Helicobacter pylori*. Nature 388
68. Tran AX, Karbarz MJ, Wang X, Raetz CR, McGrath SC, Cotter RJ, Trent MS (2004) Periplasmic cleavage and modification of the 1-phosphate group of *Helicobacter pylori* lipid A. J Biol Chem 279(53):55780-91
69. Tubau-Juni N, Bassaganya-Riera J, Leber A, Zoccoli-Rodriguez V, Kronsteiner B, Viladomiu M, Abedi V, Philipson CW, Hontecillas R (2020) Identification of new regulatory genes through expression pattern analysis of a global RNA-seq dataset from a *Helicobacter pylori* co-culture system. Scientific reports 10(1):11506
70. Turnbull KJ, Gerdes K (2017) H ic A toxin of *Escherichia coli* derepresses hic AB transcription to selectively produce H ic B antitoxin. Molecular Microbiology 104(5):781-792
71. Vallese F, Percudani R, Fischer W, Zanotti G (2015) The crystal structure of *Helicobacter pylori* HP1029 highlights the functional diversity of the sialic acid-related DUF386 family. Febs j

282(17):3311-22

72. Van Vliet A, Kuipers E, Stoof J, Poppelaars S, Kusters J (2004) Acid-Responsive Gene Induction of Ammonia-Producing Enzymes in *Helicobacter pylori* Is Mediated via a Metal-Responsive Repressor Cascade. Infection and Immunity 72:766-773
73. Vandesompele J, De Preter K, Pattyn F, Poppe B, Van Roy N, De Paepe A, Speleman F (2002) Accurate normalization of real-time quantitative RT-PCR data by geometric averaging of multiple internal control genes. Genome Biol 3(7):Research0034
74. Wen Y, Marcus Elizabeth A, Matrubutham U, Gleeson Martin A, Scott David R, Sachs G (2003) Acid-Adaptive Genes of *Helicobacter pylori*. Infection and Immunity 71(10):5921-5939
75. Wessler S, Posselt G (2024) Bacterial proteases in *Helicobacter pylori* infections and gastric disease. Helicobacter pylori and Gastric Cancer:259-277
76. White ML, Hough-Neidig A, Khan SJ, Eswara PJ (2022) MraZ is a transcriptional inhibitor of cell division in *Bacillus subtilis*. bioRxiv:2022.02. 09.479790
77. Yamaguchi Y, Inouye M (2011) Regulation of growth and death in *Escherichia coli* by toxin–antitoxin systems. Nature Reviews Microbiology 9(11):779-790
78. Yang H, Huang X, Zhang X, Zhang X, Xu X, She F, Wen Y (2022) AI-2 Induces Urease Expression Through Downregulation of Orphan Response Regulator HP1021 in *Helicobacter pylori*. Frontiers in Medicine Volume 9 - 2022
79. Yang H, Wang L, Zhang M, Hu B (2023) The Role of Adhesion in *Helicobacter pylori* Persistent Colonization. Current Microbiology 80(5):185
80. Yuan Y, Hefner Y, Szubin R, Sung J, Palsson Bernhard O (2026) Revealing transcriptomic responses in *Escherichia coli* during early antibiotic exposure. mSystems 11(4):e01584-25
81. Zanotti G, Cendron L (2014) Structural and functional aspects of the *Helicobacter pylori* secretome. World J Gastroenterol 20(6):1402-23
82. Zhao J, Wang Q, Li M, Heijstra BD, Wang S, Liang Q, Qi Q (2013) *Escherichia coli* toxin gene hipA affects biofilm formation and DNA release. Microbiology 159(Pt_3):633-640
83. Zimmerman E, Ramsey E, Hunter K, Villadelgado S, Phillips C, Shipman R, Forsyth M (2023) The *Helicobacter pylori* methylome is acid-responsive due to regulation by the two-component system ArsRS and the type I DNA methyltransferase HsdM1 (HP0463). Journal of Bacteriology 206

Table

Table 1 is available in the Supplementary Files section.

Figures

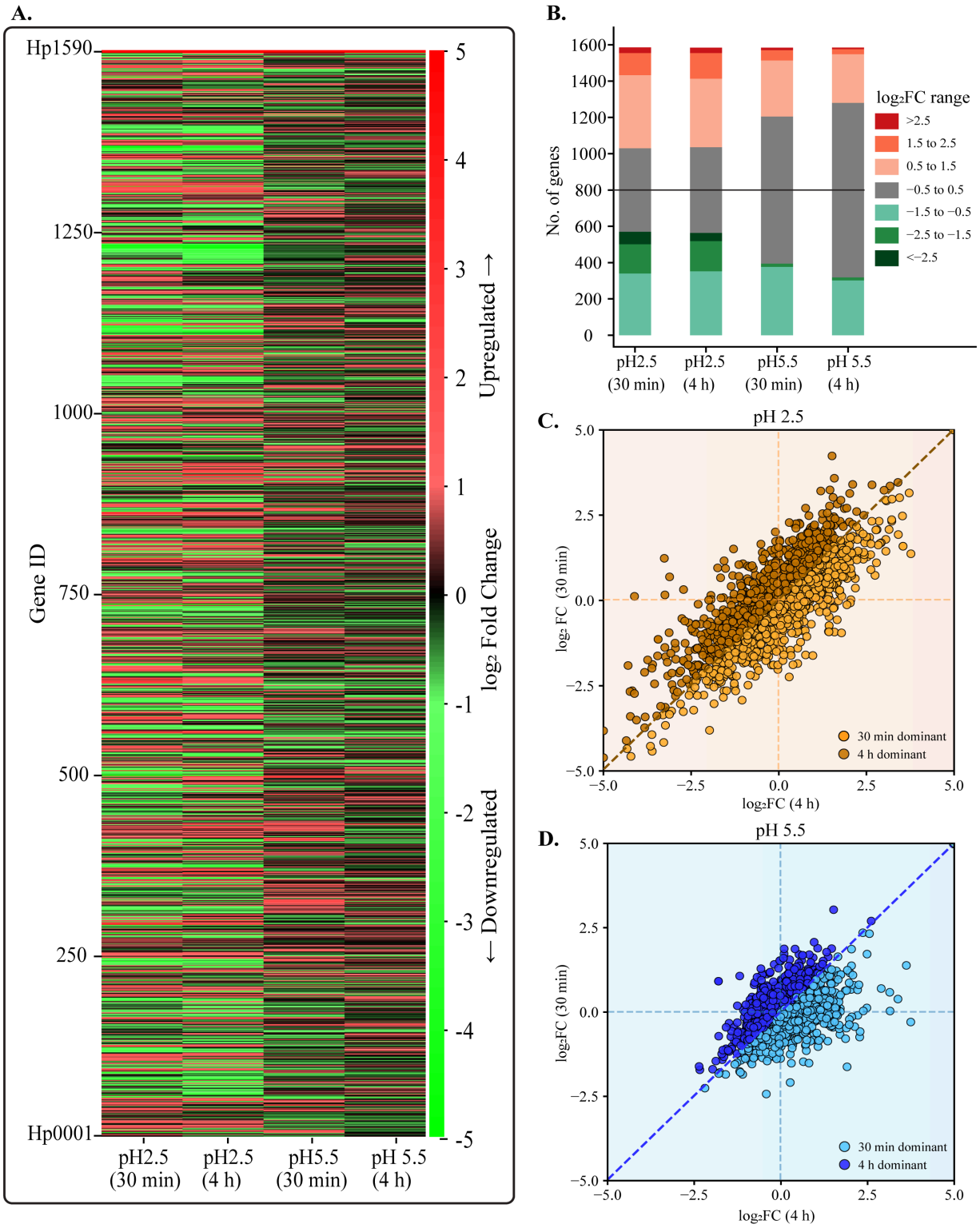


Figure 1

The transcriptional profiling of *H. pylori* 26695 under acid-stress conditions. (A) Heatmap showing the expression profiles of 1,564 *H. pylori* 26695 genes following exposure to pH 2.5 and pH 5.5 for 30 min and 4 h compared to control (pH 7.4). Gene expression is represented on a color scale, i.e. red: upregulation, green: downregulation, and black: no significant change. **(B)** Stacked bar chart showing the distribution of genes across different $\log_2$ fold-change ($\log_2$FC) intervals (≤-2.5, -2.5 to -1.5, -1.5 to -0.5,

-0.5 to 0.5, 0.5 to 1.5, 1.5 to 2.5, and ≥2.5) under different conditions. **(C, D)** Scatter plots comparing log_2FC values at 30 min and 4 h under pH 2.5 (C) and pH 5.5 (D). Each point represents an individual gene, illustrating temporal changes in gene expression in response to extreme and moderate acid stress.

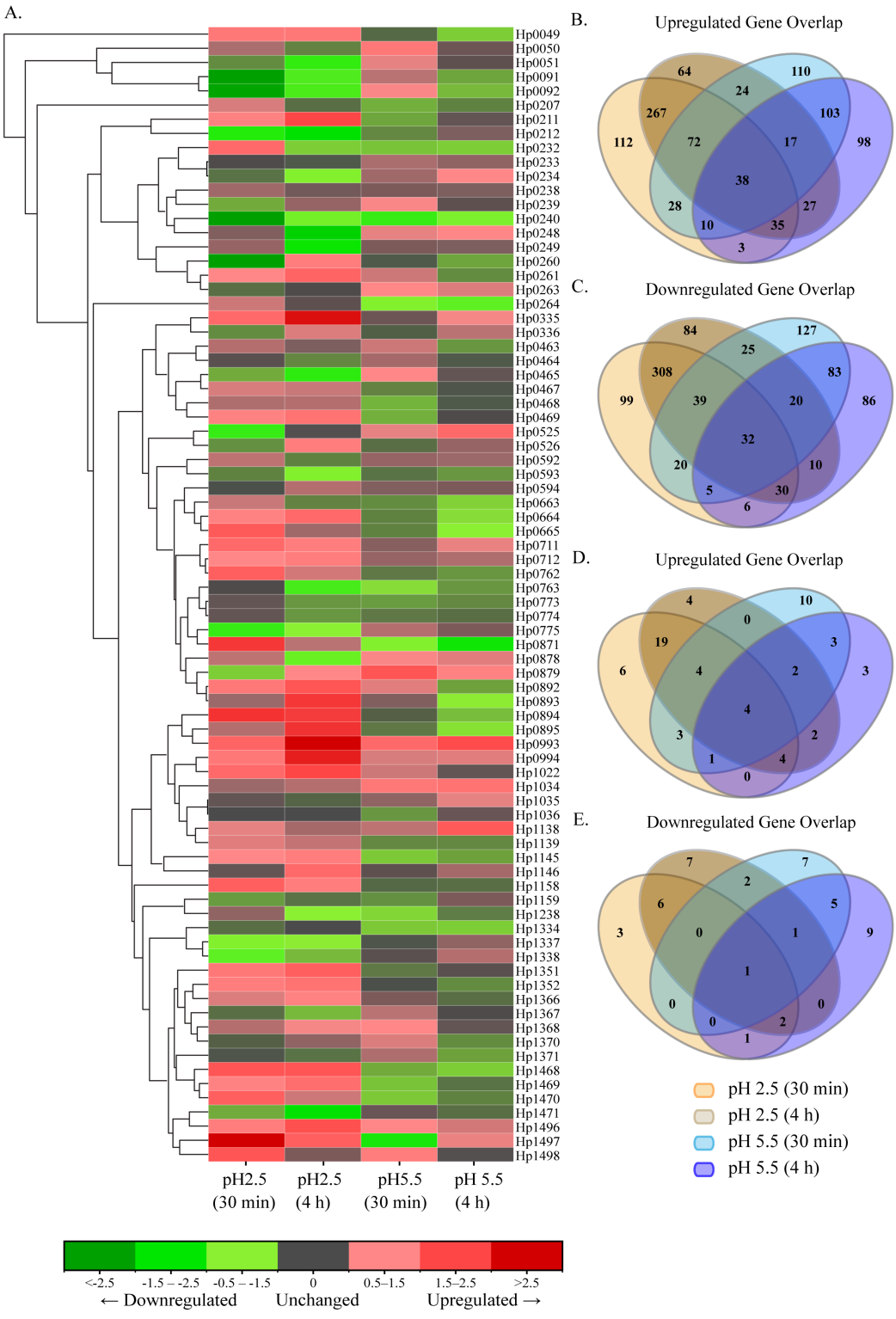


Figure 2

Heatmap of putative toxin-antitoxin genes. (A) Heatmap showing hierarchical clustering of significantly differentially expressed putative toxin-antitoxin (TA) genes of *H. pylori* 26695 under four acid stress conditions: pH 2.5 (30 min & 4 h), pH 5.5 (30 min & 4 h), compared to control (pH 7.4). The color scale represents log_2FC values, and the dendrogram indicates similarities in expression patterns among TA genes. **(B, C)** Four-way Venn diagrams of all the ORFs showing the overlap of upregulated (B) and downregulated (C) genes among the four acid stress conditions. Numbers indicate genes uniquely or commonly regulated under each condition. **(D, E)**Four-way Venn diagrams of 80 putative TA genes illustrating the overlap of upregulated (D) and downregulated (E) genes among the four acid stress conditions.

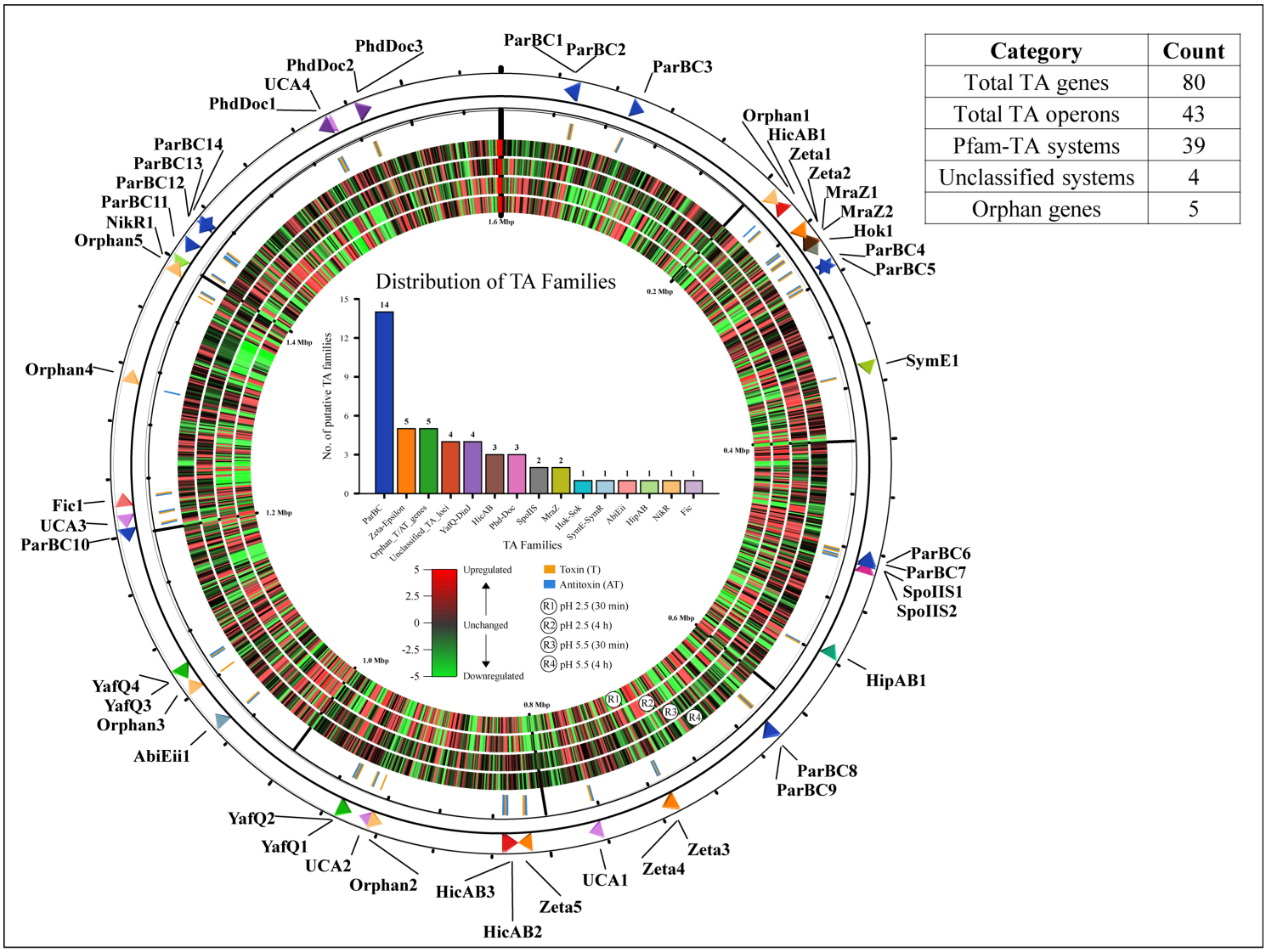


Figure 3

Genome-wide distribution and expression profiling of putative toxin-antitoxin systems in *H. pylori* 26695. Circular map showing the genomic distribution and orientation of predicted toxin-antitoxin (TA) loci in *H. pylori* 26695 (NC_000915). Outer tracks represent coding sequences on the forward and reverse strands. Inner concentric rings display normalized expression values (log_2 FC) under four acid

stress conditions: pH 2.5, 30 min & 4 h, pH 5.5, 30 min & 4 h compared to control (pH 7.4). Red, green, and black indicate upregulation, downregulation, and no significant change, respectively. Toxin (T) and antitoxin (AT) genes are indicated at their corresponding genomic positions. The inset summarizes the distribution of predicted TA families identified in *H. pylori* 26695, with the number of loci shown for each family.

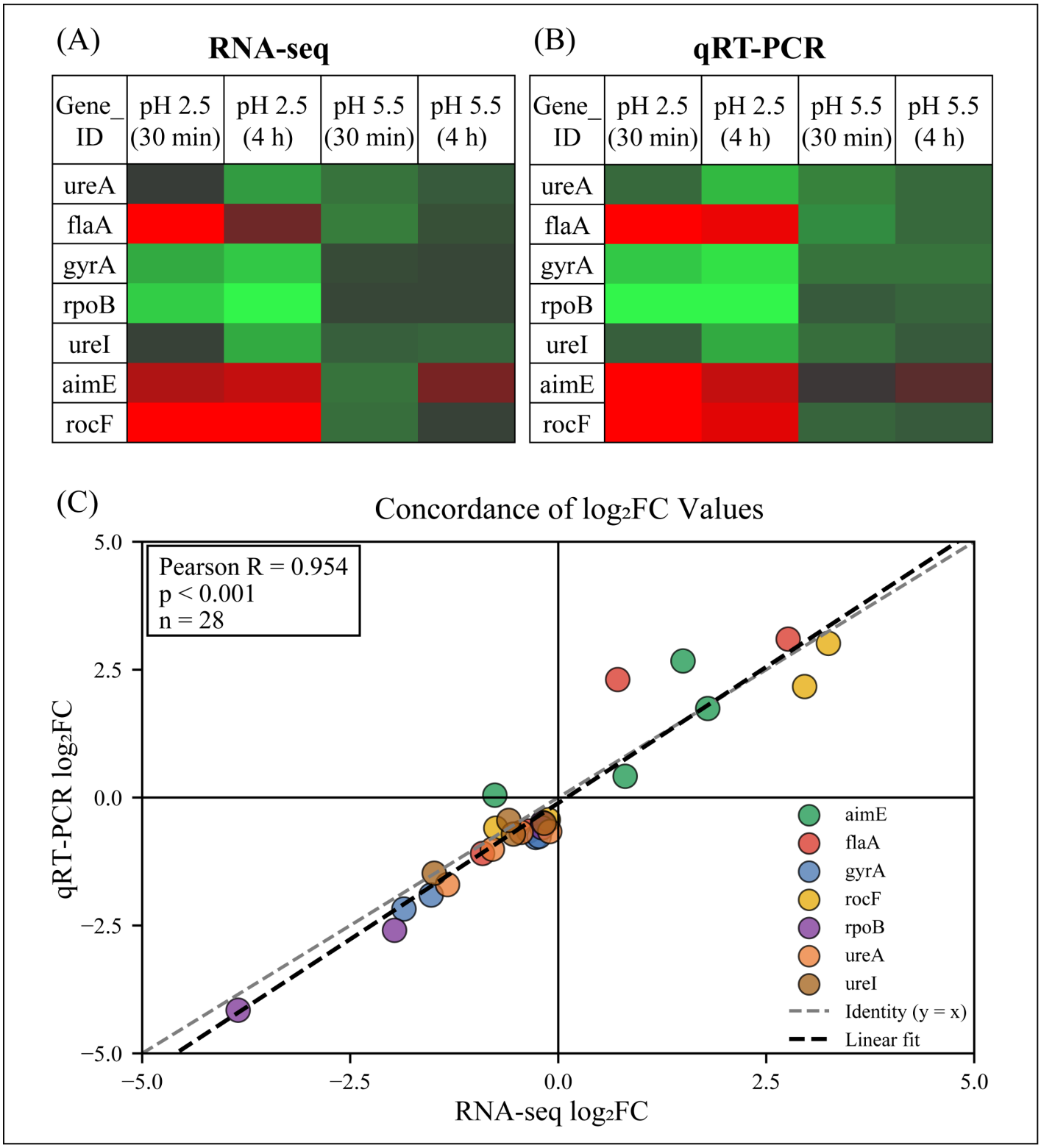


Figure 4

Validation of RNA-seq expression profiles using functionally characterised control genes. Heatmaps showing log_2 FC values relative to pH 7.4 control determined by **(A)**RNA-seq and **(B)** qRT-PCR for seven *H. pylori* 26695 control genes; ureA (Hp0073), flaA (Hp0601), gyrA (Hp0701), rpoB (Hp1198), ureI (Hp0071), aimE (Hp0294), and rocF (Hp1399) under four acid stress conditions. Red, green and black indicate upregulation, downregulation and unchanged expression, respectively. **(C)** Scatter plot showing the relationship between RNA-seq and qRT-PCR log_2FC values for all genes and conditions (n = 28). Points are color-coded by gene. The black dashed line represents the linear regression, and the grey dotted line denotes the identity line (y = x). Pearson correlation analysis showed a strong positive correlation (R = 0.954, p < 0.001). The qRT-PCR values were calculated using the 2^(-ΔΔCt) method with the geometric mean of 16S and 23S rRNA as the normalization reference.

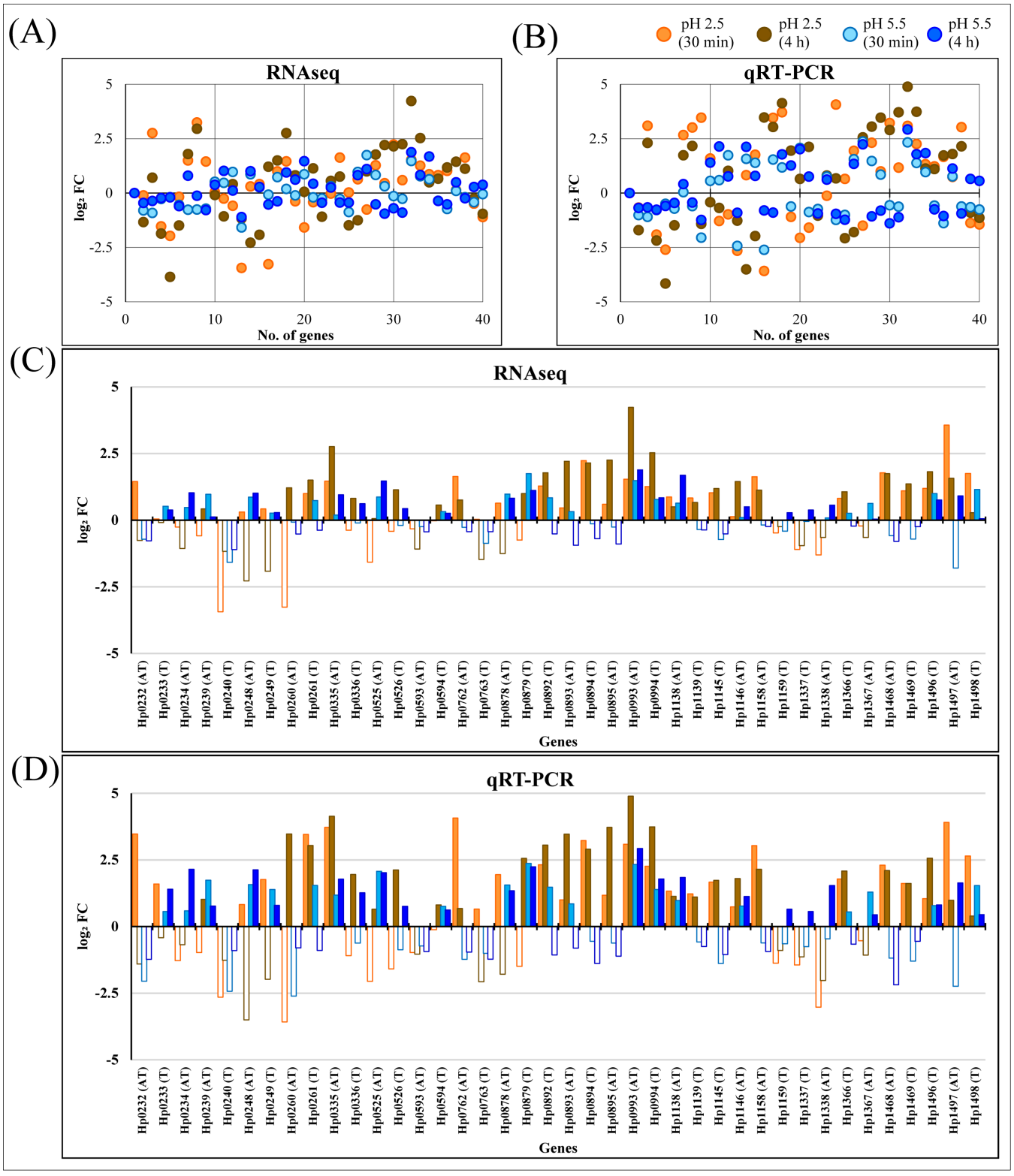


Figure 5

qRT-PCR validation of RNA-seq derived expression profiles of the toxin-antitoxin genes under acid stress. (A, B) Scatter plots showing log_2FC values of 40 toxin (T) and antitoxin (AT) genes belonging to 21 putative TA operons in *H. pylori* 26695, as determined by (A) RNA-seq and (B) qRT-PCR under four acid stress conditions compared to control (pH 7.4). **(C, D)** Gene-wise bar plots showing log_2 FC values

of the same 40 TA genes obtained by **(C)** RNA-seq and **(D)** qRT-PCR. Colours indicate stress conditions: pH 2.5 (30 min), orange; pH 2.5 (4 h), dark brown; pH 5.5 (30 min), light blue; and pH 5.5 (4 h), dark blue.

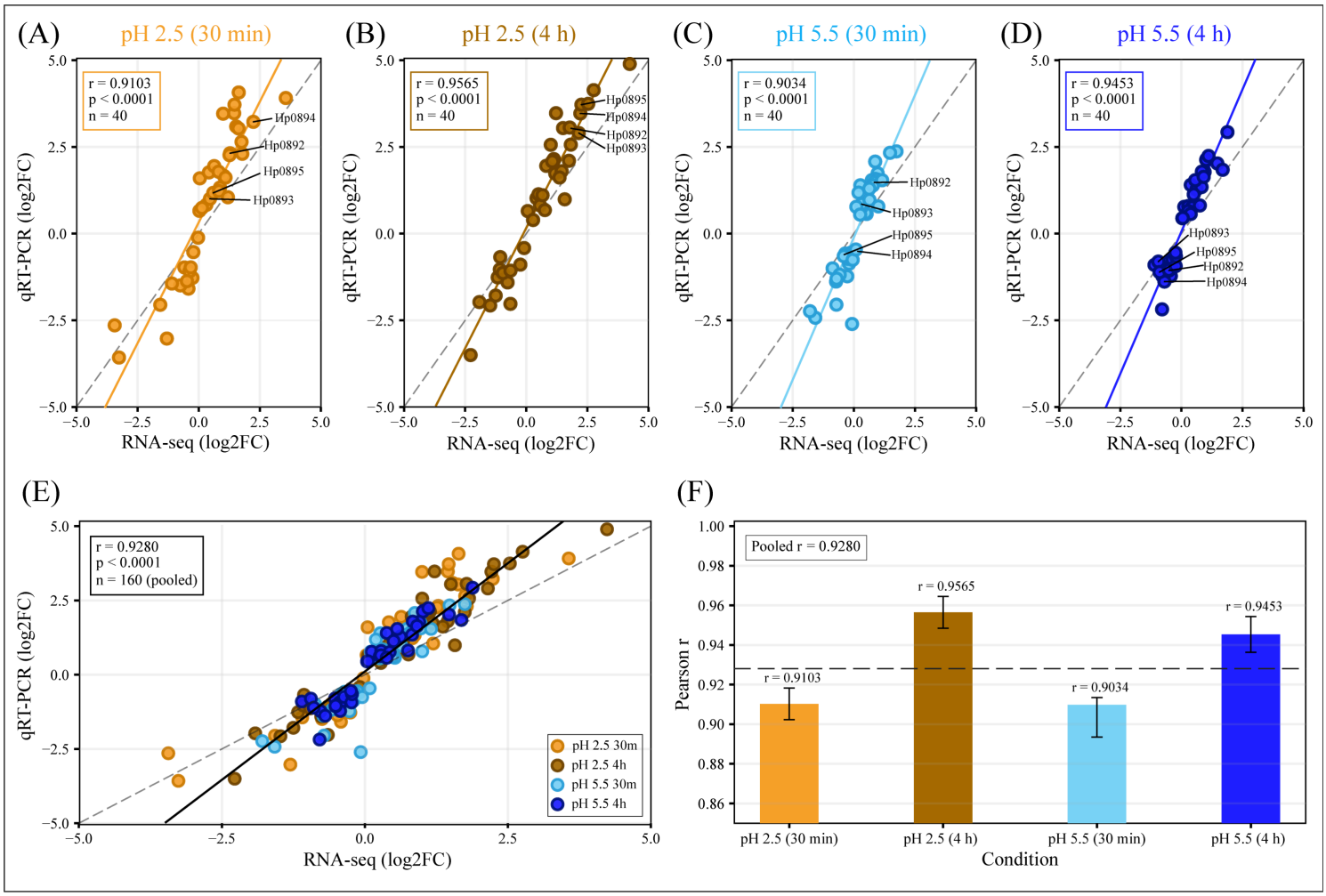


Figure 6

Correlation between RNA-seq and qRT-PCR expression profiles of individual toxin-antitoxin genes under acid stress. Scatter plots showing the relationship between qRT-PCR-derived $\log_2$ FC values (y-axis) and RNA-seq-derived $\log_2$ FC values (x-axis) for 40 toxin (T) and antitoxin (AT) genes from 21 putative TA operons of *H. pylori* 26695 under **(A)** pH 2.5 (30 min), **(B)**pH 2.5 (4 h), **(C)** pH 5.5 (30 min), and **(D)** pH 5.5 (4 h). Each panel displays the Pearson correlation coefficient (r), p-value, and number of observations (n = 40). The solid line represents the linear regression, the shaded region denotes the 95% confidence interval, and the dashed line indicates the identity line (y = x). **(E)** Pooled correlation analysis comprising all 160 observations (40 genes × 4 conditions), colour-coded according to acid stress conditions: pH 2.5 (30 min: orange; 4 h: dark brown); pH 5.5 (30 min: light blue; 4 h: dark blue). The pooled Pearson correlation coefficient was r = 0.9280 ($p < 0.0001$). **(F)** Comparison of Pearson correlation coefficients obtained for each condition. Error bars indicate the 95% confidence intervals, and the dashed line represents the pooled correlation coefficient (r = 0.9280).

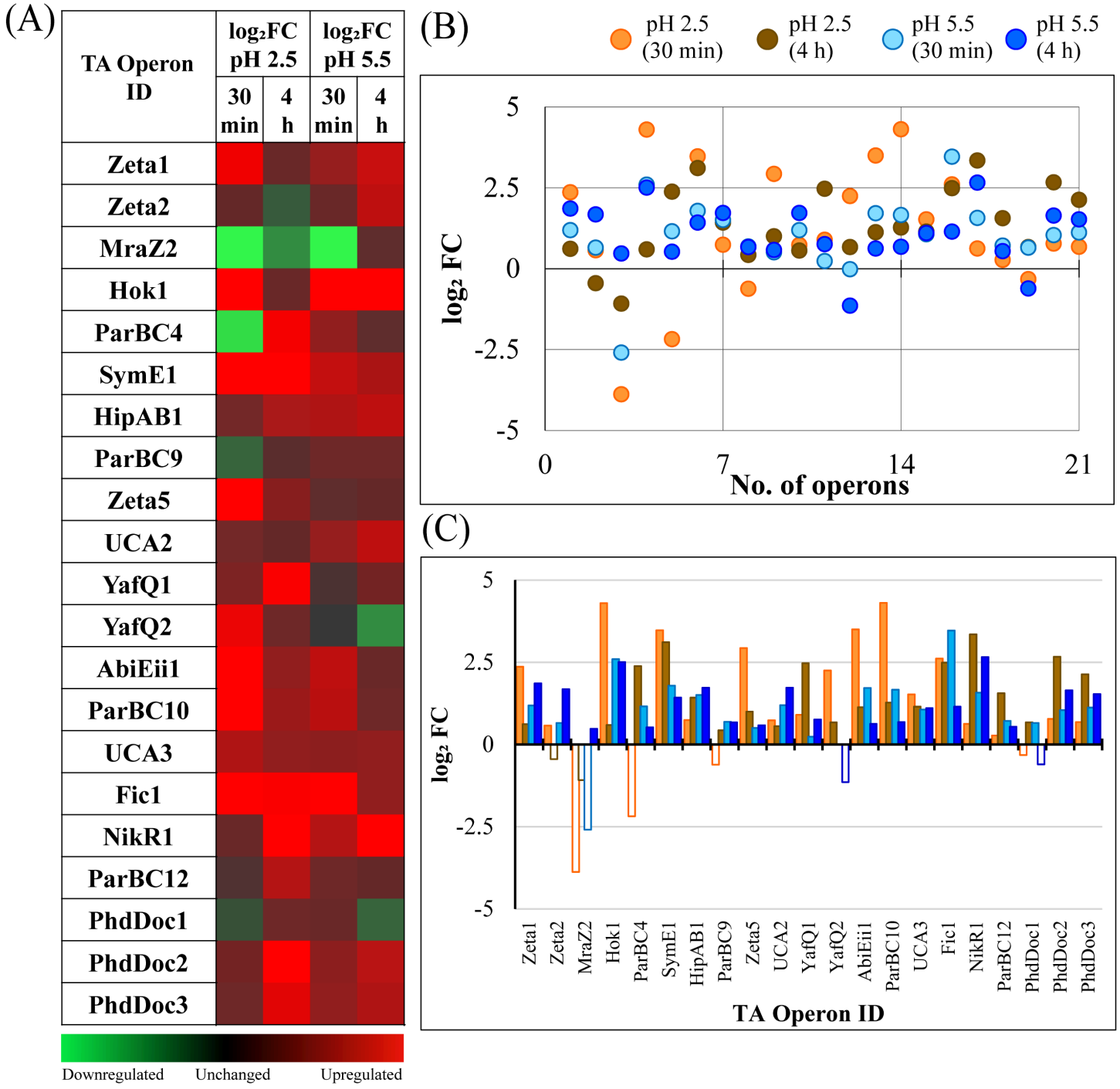


Figure 7

qRT-PCR analysis of toxin-antitoxin operon expression under acid stress conditions.
(A) Heatmap showing operon level log_2FC value of 21 selected TA operons under four acid stress conditions (pH 2.5, 30 min & 4 h), pH 5.5, 30 min & 4 h) compared to control (pH 7.4). Expression values were normalized using the geometric mean of 16S and 23S rRNA Ct values. Red, green and black indicates upregulation, downregulation and unchanged respectively. **(B)**Scatter plot showing the distribution of operon-level log_2FC values under each condition. **(C)** Gene-wise bar plots of the 21 TA operons.

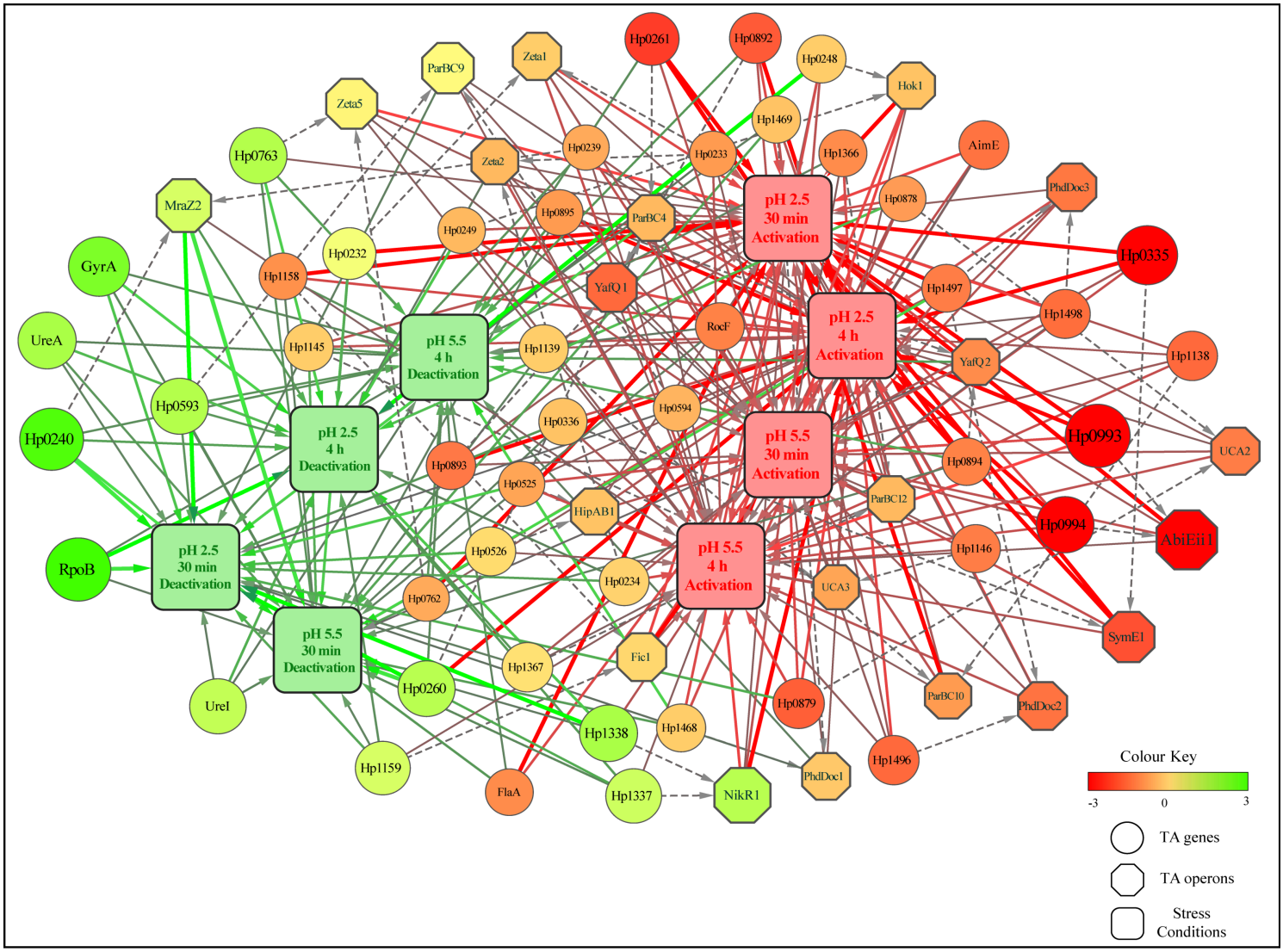


Figure 8

Network visualization of toxin-antitoxin genes and operons under acid stress. Integrated network showing the relationships among individual toxin-antitoxin (TA) genes (circular nodes), TA operons (octagonal nodes), and acid stress conditions (square nodes) in *H. pylori* 26695 exposed to pH 2.5 and pH 5.5 for 30 min and 4 h. Node colours indicate expression levels based on qRT-PCR-derived $\log_2$ FC values relative to pH 7.4, with red representing upregulation, green representing downregulation, and yellow indicating little or no change. Red and green edges denote activation and deactivation relationships, respectively, and edge thickness corresponds to the magnitude of expression change. Condition nodes are classified according to pH and exposure time. The network was generated using qRT-PCR-validated expression data.

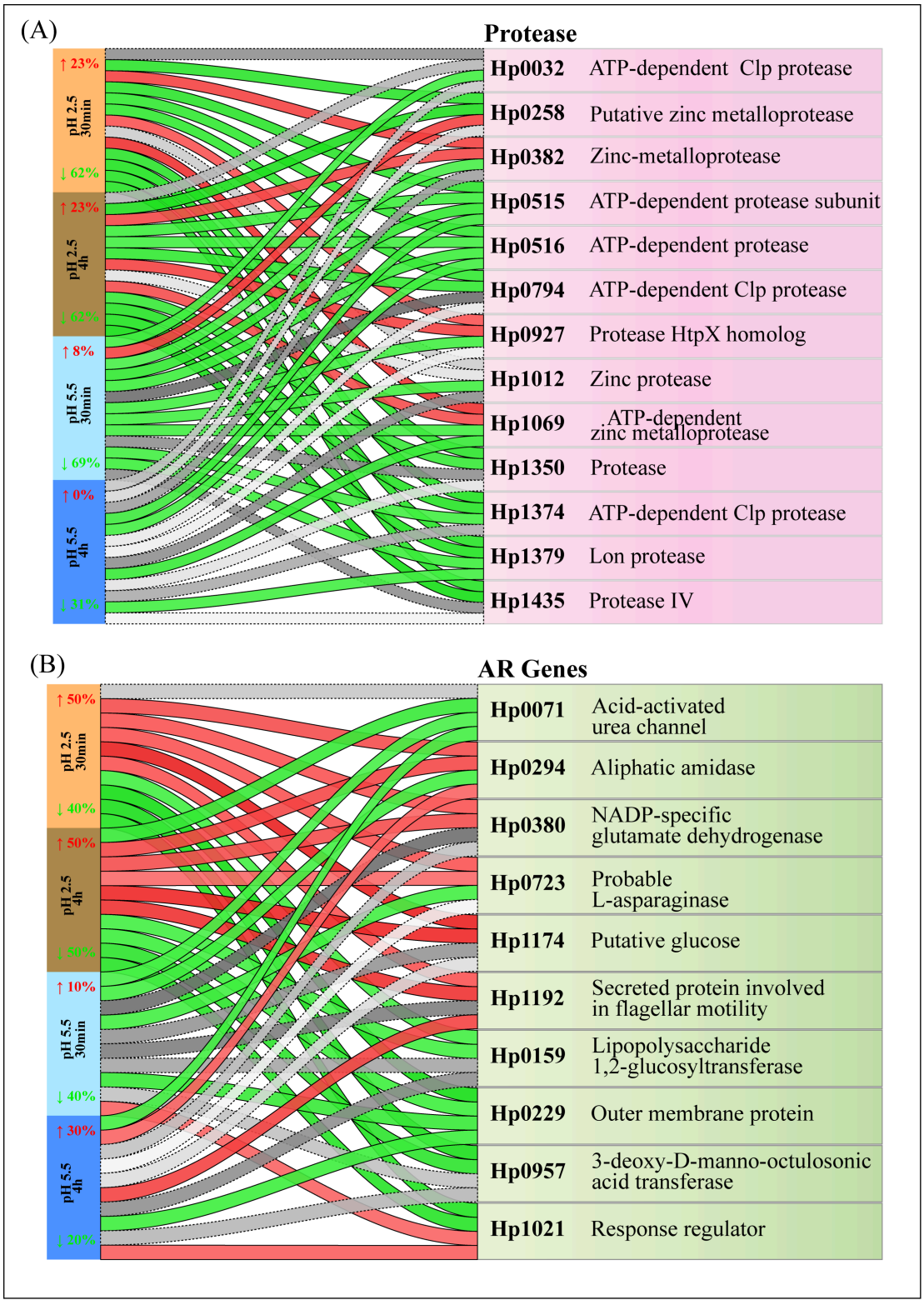


Figure 9

The expression profiles of protease and acid-resistance genes in *H. pylori* 26695 under acid stress. Sankey flow charts showing the distribution of transcriptional responses of **(A)** 13 protease-encoding genes and **(B)**10 acid-resistance (AR) associated genes under four acid stress conditions (pH 2.5, 30 min & 4 h), pH 5.5, 30 min & 4 h) relative to the physiological control (pH 7.4). Red, green and grey indicate upregulation, downregulation and unchanged expression respectively, according to their RNA-

seq $\log_2$ FC values. The percentages shown on the left indicate the proportion of genes in each expression category for a given condition, whereas the width of each flow corresponds to the relative contribution of genes to that category. Gene identities and functional annotations are listed on the right.

Supplementary Files

This is a list of supplementary files associated with this preprint. Click to download.

- 01SupplementaryData.pdf
- Tabl1.png